1984

Directional solidification studies of Pb-Bi peritectic alloys

Bor-Ching Fuh
Iowa State University

Fuh, Bor-Ching

DIRECTIONAL SOLIDIFICATION STUDIES OF LEAD-BISMUTH PERITECTIC ALLOYS

Iowa State University PH.D. 1984

PLEASE NOTE:

In all cases this material has been filmed in the best possible way from the available copy. Problems encountered with this document have been identified here with a check mark _✓_.

1. Glossy photographs or pages _____
2. Colored illustrations, paper or print _____
3. Photographs with dark background _✓_
4. Illustrations are poor copy _____
5. Pages with black marks, not original copy _____
6. Print shows through as there is text on both sides of page _____
7. Indistinct, broken or small print on several pages _____
8. Print exceeds margin requirements _____
9. Tightly bound copy with print lost in spine _____
10. Computer printout pages with indistinct print _____
11. Page(s) _____ lacking when material received, and not available from school or author.
12. Page(s) _____ seem to be missing in numbering only as text follows.
13. Two pages numbered _____. Text follows.
14. Curling and wrinkled pages _____
15. Other _____

Directional solidification studies of Pb-Bi peritectic alloys

by

Bor-Ching Fuh

A Dissertation Submitted to the
Graduate Faculty in Partial Fulfillment of the
Requirements for the Degree of
DOCTOR OF PHILOSOPHY

Department: Materials Science and Engineering
Major: Metallurgy

Approved:

Signature was redacted for privacy.

In Charge of Major Work

Signature was redacted for privacy.

For the Major Department

Signature was redacted for privacy.

For the Graduate College

Iowa State University
Ames, Iowa

1984

TABLE OF CONTENTS

GENERAL INTRODUCTION

During the past thirty years, many theoretical and experimental studies have been carried out to predict the interface morphology and solute distribution during the controlled solidification of binary alloys. However, most of these studies are carried out on eutectic systems. In recent years, controlled solidification of peritectic alloys has been receiving a great deal of attention and has been the subject of detailed analytical and experimental studies. The peritectic reaction involves the combination of a solid (α) and liquid (L) phase to form a different solid (β) phase on solidification. The reaction is isothermal in binary alloys and is illustrated in Figure 1. When the second phase forms, it surrounds the first solid phase and the peritectic reaction can proceed only by diffusion of solute through the second phase. In general, the first solid phase will be formed as dendrites. Somewhere behind the dendrite tips, partial reaction with the interdendritic liquid occurs to give the peritectic phase. The microstructure of these alloys is, therefore, dendritic for the peritectic phase, and an eutectic phase often forms in the interdendritic region. The most important commercial material that solidifies with the peritectic reaction is carbon steel. A number of directional solidification studies have been carried out to study the primary phase and the peritectic phase for alloys of peritectic composition [1-14]. There are some important aspects of solidification structures in peritectic systems which are still not

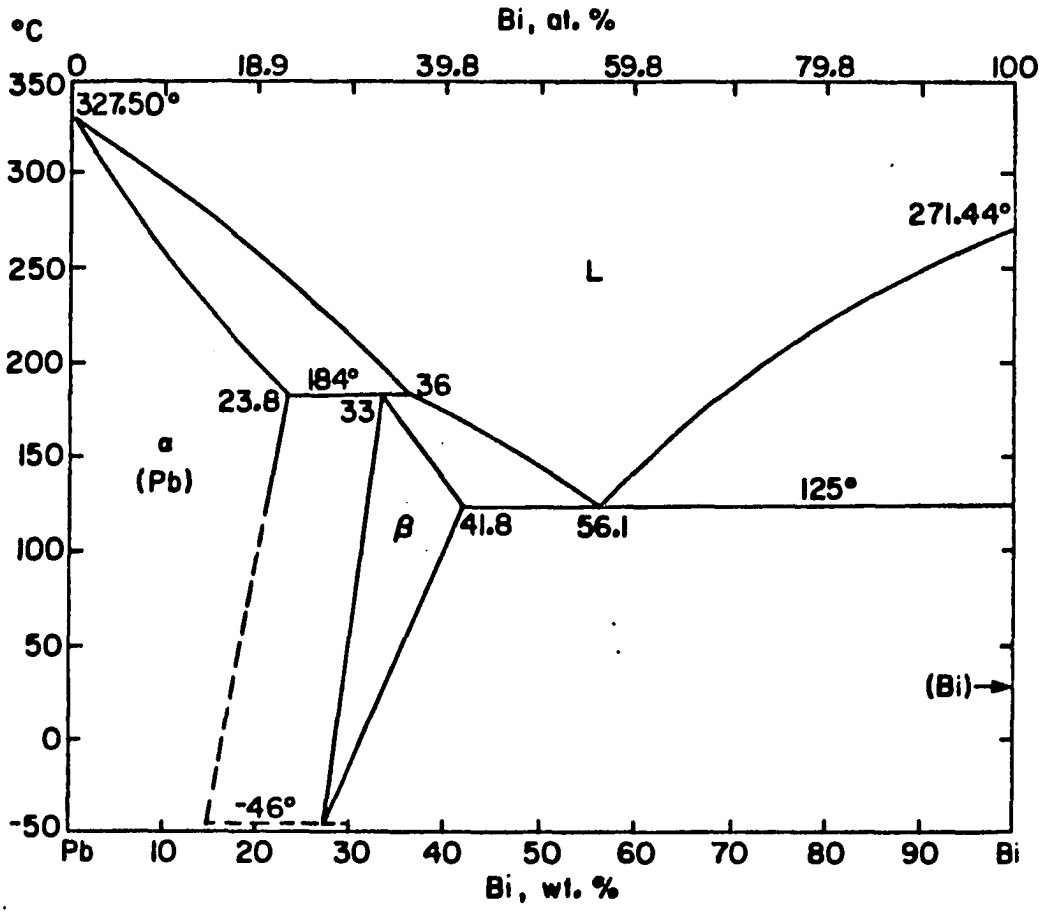

Figure 1. Lead-bismuth phase diagram. The peritectic reaction occurs at 184°C, and the reaction is $\alpha(23.8) + \text{Liq.}(36) \rightarrow \beta(33)$

well-understood.

1) In the peritectic system (shown in Figure 1), α-phase forms as dendrites with the β-phase forming in the interdendritic region. Chalmers [15] has suggested that, under some experimental conditions, it should be possible to grow α and β phases cooperatively as in the case of the eutectic reaction. A number of experimental studies reported in the literature have failed to show the cooperative growth phenomenon. We plan to carry out a few critical experiments to investigate the cooperative growth phenomenon.

2) For a given alloy composition, a transition in structure from the α phase to the β phase is observed. This transition is a function of growth velocity (V) and temperature gradient (G) in liquid. We plan to carry out directional solidification studies at which α to β transition occurs. These studies will also be extended to characterize primary dendrite spacings of α dendrites and β dendrites.

3) Some experimental studies show that solidification structures in peritectic systems often occur as alternate bands of the two phases. However, there is as yet no clear agreement on the interpretation of the band microstructures. Our aim is to determine experimental conditions under which such a band formation can occur.

The characteristics of crystals are governed by the alloy of impurity composition (C_∞), the growth velocity (V) and the temperature gradient at the interface (G). In order to separate the effect of each of these variables, controlled solidification studies will be carried out on alloys of different compositions. In these experiments,

both the growth rate and the temperature gradient in liquid may be independently controlled so that we can study the crystal growth characteristics as a function of either the temperature gradient (at constant growth rate) or the velocity (at constant growth rate). There are several methods of heat extraction. Figure 2a shows directional solidification where the crucible is drawn downwards through a constant temperature gradient at a uniform rate, V, and therefore, the microstructure is highly uniform throughout the specimen. Figure 2b shows directional casting. The benefits of directionality, such as a better control of the properties and an absence of detrimental macrosegregation, are retained, but the microstructure is no longer uniform along the specimen because the growth rate and the temperature gradient decrease as the distance from the chill increases. The present studies will be carried out under directional solidification conditions where each individual experimental variable can be isolated and its influence on peritectic structure examined.

The first section is a report on the results of the α to β phase transition in lead-bismuth peritectic alloys at low growth rate and at high growth rate. The critical growth rates at which the α-phase and β-phase growth at the same front under a series constant temperature gradients and compositions have been determined. The second section deals with the results of the primary cell and dendrite spacings in lead-bismuth systems as a function of compositions (C), growth rates (V) and temperature gradient in liquid (G) of peritectic alloys and hypoeutectic alloys. The third section deals with the band structure

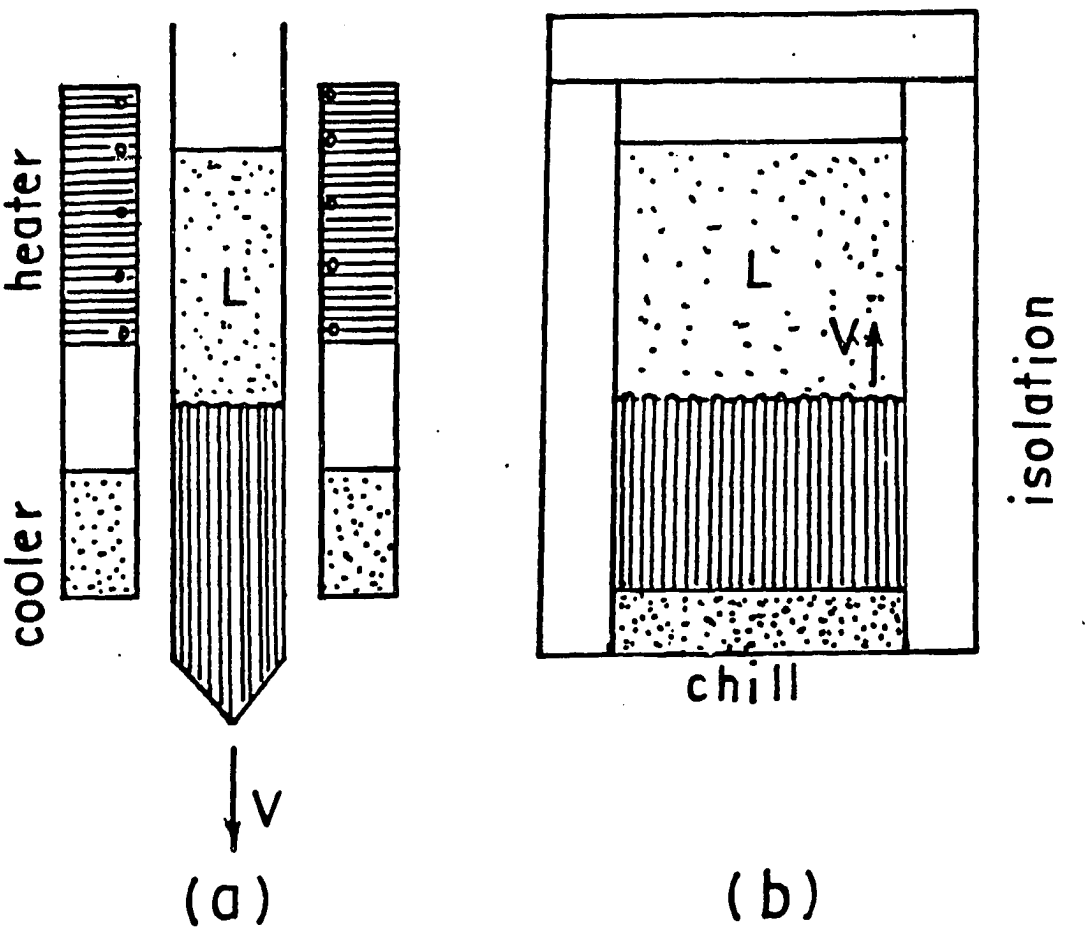

Figure 2. Basic methods of controlled solidification

in Pb-Bi peritectic alloys. An explanation for the band structures formation in Pb-Bi peritectic alloys will be proposed in this section.

SECTION I. $\alpha \rightarrow \beta$ PHASE TRANSITION IN Pb-Bi PERITECTIC ALLOYS

INTRODUCTION

One of the interesting transitions in structures as a function of solidification rate occurs in peritectic systems. An alloy near the peritectic composition generally solidifies with the formation of α dendrites. However, as the solidification rate is reduced below a certain rate, the same alloy freezes with a planar β phase interface [1-3]. In comparison with the dendrite-eutectic transition results [4], one could also expect a transition from α dendrites to β dendrites above a certain value of the velocity. Such a high rate is commonly encountered in high speed welding. Since many commercially important alloys exhibit peritectics, such a structural transition has very important technological implications, e.g., the austenite to ferrite dendrite transition in austenitic stainless steels welded at high speeds. Our aim in this paper is to examine the high velocity transition and to characterize α to β transition at low velocity in the Pb-Bi system. Furthermore, a number of experimental studies on the directional solidification of peritectic alloys [1-10] have shown that peritectic phases α and β, unlike eutectic, cannot be grown cooperatively. We will also examine if certain conditions exist at which a planar peritectic interface will result in which both α and β phases grow cooperatively, as suggested by Chalmers [11].

In this paper, we shall present the results of directional solidification studies carried out over a wide range of velocity, temperature gradient and composition. Microstructural changes, as well

as interface temperatures, were measured near the $\alpha \rightarrow \beta$ transition conditions. Our experimental studies have shown that α to β transitions occur at very low velocities and at very high velocities. Furthermore, a cooperative growth of α and β phase has been observed, and a relationship between the velocity, temperature gradient and composition is obtained for which such a cooperative growth occurs. The high velocity $\alpha \rightarrow \beta$ transition was found to agree with the theoretical model proposed in this paper. The low velocity $\alpha \rightarrow \beta$ transition, and the cooperative growth phenomenon, were found to be strongly influenced by convection effects which were shown to be present at very low velocities.

THEORETICAL BACKGROUND

Mollard and Flemings [1] and Rinaldi *et al.* [2] have found that a simple constitutional supercooling stability criterion approximately describes the stability of multiphase planar liquid-solid interfaces in eutectic alloy systems. Brody and David [3] applied it to describe the stability of a planar interface in a peritectic alloy system. This criterion states that; for S_1 (Figure 1a):

$$D_L \frac{G}{V} = m_1 C_o \frac{(1-k_1)}{k_1} \quad . \tag{1}$$

For S_2:

$$D_L \frac{G}{V} = m_2 C_o \frac{(1-k_2)}{k_2} \tag{2}$$

where D_L, G and V are the diffusion coefficient in liquid, temperature gradient and velocity, respectively. C_o is the solute content of the alloy, and m and k are the slope of the liquidus and the equilibrium partition coefficient, respectively. The results of Equations (1) and (2) are plotted as lines oa and obc in Figure 1 using the values of m_1, m_2, k_1, and k_2 which are defined by the schematic phase diagram. The condition for suppressing the S_1 dendrite tips below the peritectic temperature, which is the equilibrium solidus for compositions between C_1 and C_2, was obtained by using the result of Bower *et al.* [4]. The result is

$$\Delta T = D_L \frac{G}{V} > m_1 (C_L - C_o) \tag{3}$$

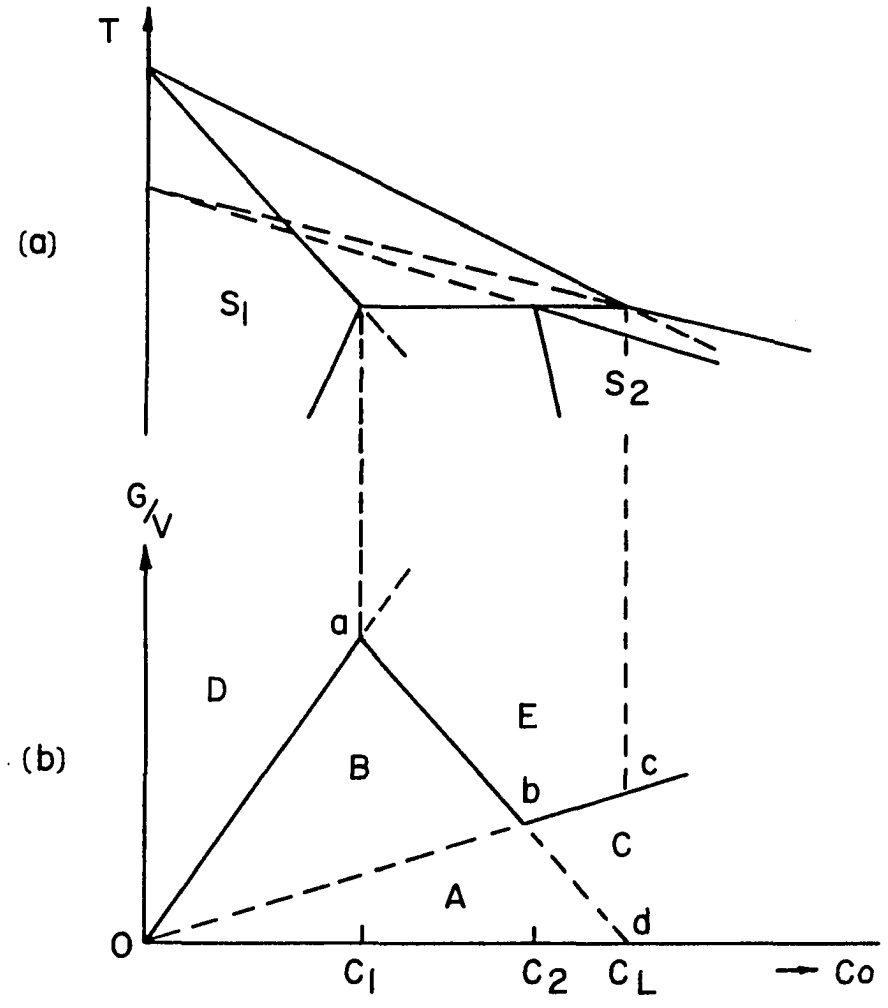

Figure 1. A typical phase diagram of a peritectic system and critical G/V vs. C_o plot to obtain a planar solid/liquid interface. Expected microstructures and interface morphology are also shown as: A-primary dendrites of S_1 surrounded by S_2; B-rods of S_1 followed by planar S_2; C-cellular or dendritic S_2; D-single phase planar S_1; and E-single phase planar S_2. (From reference [3])

where ΔT is the difference between the liquidus and peritectic temperatures. This relationship is plotted as abd in Figure 1b. In this figure, the region A represents freezing conditions at small values of G/V. Here, dendrites of the primary phase S_1 would grow ahead of the peritectic iostherm and be surrounded by gradually thickening S_2 below the peritectic isotherm. For higher values of G/V, in Region B, primary dendrites or cells of S_1 will grow with higher undercoolings at the tips and S_2 will freeze at a plane front at the peritectic temperature. For higher initial solute contents, in Region C, S_2 will grow with either a dendritic or cellular interface. For still higher values of G/V, in Regions D and E, a single phase material will grow with a planar front. Experimental results for Pb-Bi system have been found to give good agreement with the boundaries separating the morphological behavior of the alloys [3].

According to the above analysis of Brody and David [3], the α to β phase transition occurs along the conditions represented by the line ab. There are two major drawbacks to their analysis. (1) For a given composition, an α to β transition is predicted for a unique velocity. However, from our understanding of the dendrite to eutectic transition, we would expect the α to β transition to occur at low, as well as high, velocities. (2) The transition line ab is calculated on the basis that β phase will form only if the interface temperature is at the peritectic temperature. This is indeed valid for the case considered by Brody and David in which the alloy was at the peritectic composition. However, for hypoperitectic alloys, it has been found by St. John and

Hogan [12] that the temperature of the β phase is higher than the peritectic temperature. Precisely what undercooling is required to form stable β phase cannot be predicted by the simple analysis used to obtain Equation (3).

A better theoretical model would be to use the idea proposed by Jackson and Hunt [13] for the dendrite to eutectic transition. If one can calculate the interface temperatures for the α and the β phase for a given experimental condition, then the phase that will be stable will be the one that has a higher interface temperature. Burden and Hunt [5] have used this criterion to show that a eutectic phase will be stable in two velocity regimes; at very low velocities and at very high velocities. We shall now examine if this criterion can be used to predict the α to β transition in peritectic systems.

The interface temperatures of the α and β phases have been calculated using the theoretical model of Trivedi [8] for the dendrite growth process. Figure 2 shows the temperature profiles for the α and β phase as a function velocity at G = 26.5 K/mm in Pb-Bi alloys of compositions 30, 33 and 35 wt.% Bi. The result shows that α phase is stable only within a band of velocities (V_1 and V_2). Below V_1 and above V_2, stable β-phase should be observed. The high velocity transition occurs at lower velocities as the composition of the alloy is increased. For Pb - 35 wt.% Bi, $V_2 \simeq 100$ μm/s. A transition at this velocity would be easy to confirm by directional solidification studies. We shall show experimentally that such a transition occurs.

Figure 2. The theoretical tip temperature versus growth rates at G = 26.5 K/mm with alloy composition (in wt.% Bi): a) 30, b) 33, and c) 35

(a)

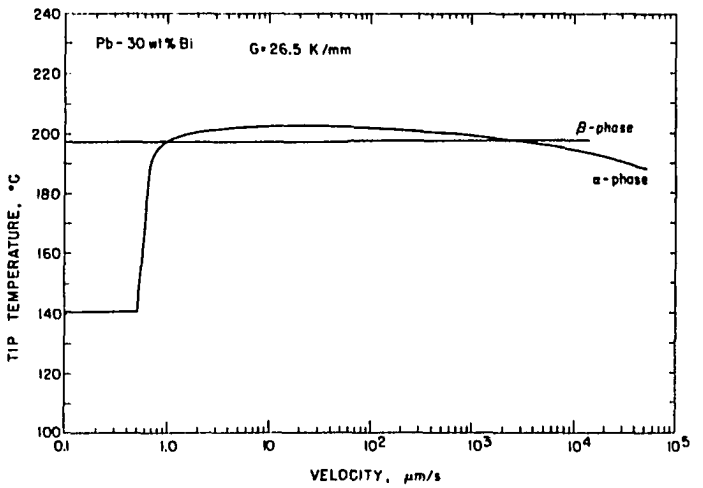
Pb - 30 wt % Bi
G = 26.5 K/mm
β-phase
α-phase
TIP TEMPERATURE, °C
VELOCITY, μm/s

(b)

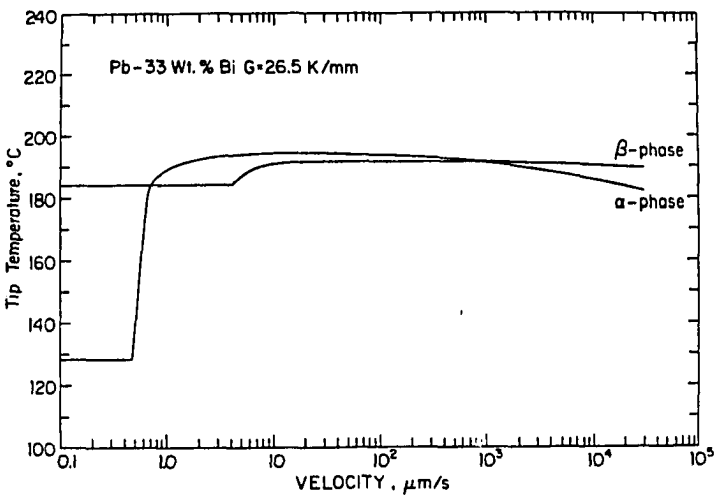
Pb-33 Wt. % Bi G=26.5 K/mm
β-phase
α-phase
Tip Temperature, °C
VELOCITY, μm/s

(c)

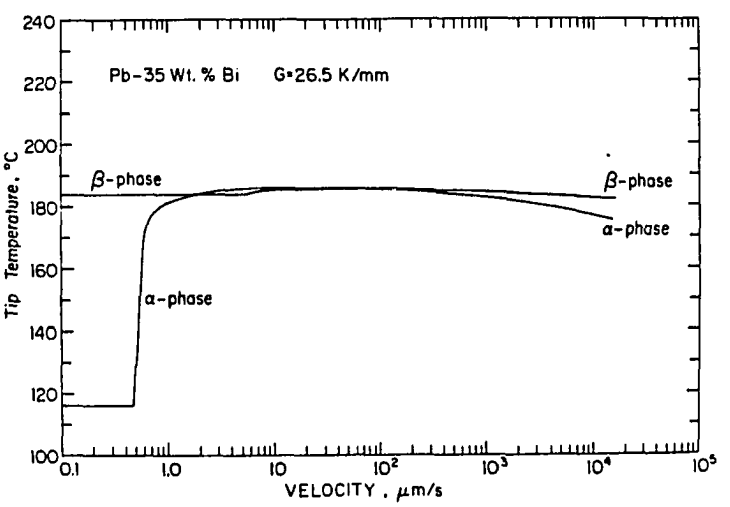
Pb-35 Wt. % Bi G=26.5 K/mm
β-phase
β-phase
α-phase
α-phase
Tip Temperature, °C
VELOCITY, μm/s

The low velocity transition is analogous to that observed by Brody and David [3]. However, three important aspects must be first realized. (1) The present model calculates the interface temperatures upon the assumption that α phase or β phase is growing independently, since when α-phase dendrites or cells form, β-phase interface is observed between the α dendrites or cells. Thus, if the length of α-cell or dendrite is small, the interaction between the α and β phase would be significant. This interaction would be largest near the critical velocity, V_1. Furthermore, the interaction will be significant when interdendritic β phase is planar since the diffusion field ahead of the planar β phase would be quite large at low velocities. The diffusion field ahead of the eutectic front is of the order of a eutectic spacing and thus, would not interact strongly with the solute field near the dendrite tip. However, for peritectic systems, the long range interaction would cause V_1 to differ significantly from the value calculated on the basis of Figure 2. (2) For interdendritic eutectic, the temperature at which the eutectic front is present is fixed by the eutectic temperature since the undercooling at low velocities is quite negligible. For peritectic systems, interdendritic β phase can form over a range of temperatures. What precisely determines the location of β phase is not yet well understood. It is thus necessary to carry out experimental studies to understand the criterion which establishes the β phase temperature when α phase dendrites or cells form. (3) The low velocity transition occurs at extremely low velocities where convection effects become significant if the experiments are carried out

in a system in which density driven solute convection occurs. Consequently, convection effects should be taken into account for predicting the transition velocity V_1.

EXPERIMENTAL TECHNIQUES

Material Preparation

Master alloys were prepared from 99.999 wt.% lead and 99.99-99.999 wt.% bismuth. The lead was cleaned in an ammonium molydate-nitric acid-water solution, then washed in distilled water and acetone before using. Preweighed amounts of the pure metals, within 0.05% of the desired composition, were placed in a clean Pyrex crucible. The crucible was transferred to a vacuum chamber which was then evacuated. The charge was melted at about 400°C by a resistance furnace and the pressure in the chamber was maintained at about 5×10^{-5} torr. When the melting was complete, a tantalum stirring rod with an attached paddle was lowered into the melt and oscillated to ensure complete mixing. The melt was then left undisturbed for approximately ten minutes and then restirred immediately before casting. In the casting operation, a bundle of 5 mm I.D./7 mm O.D. Pyrex tubes 40 cm long with one end sealed and the other end reduced in diameter were lowered to the bottom of the melt. The vacuum valve was closed and then the system was quickly backfilled with argon, thereby forcing the molten alloy up into the tubes. The alloy rapidly solidified in the Pyrex tubes and the furnace was then removed allowing the system to cool. The master alloys cast in the 5 mm I.D. Pyrex tubes were then used as samples for all subsequent work. After breaking the alloy out of the tubes and cleaning in acetone, one cast alloy sample was sectioned and chemically analyzed to determine the extent of macrosegregation. The desired

composition was Pb-29.99 wt.% Bi, and the chemical analysis results, given in wt.% Bi, were: top = 29.74, center = 29.42 and bottom = 29.83. Alloy samples 15 $\pm$ 0.5 cm long x 5 mm O.D. were used in the directional solidification studies.

Experimental Apparatus

The unidirectional solidification apparatus used in this study has been described in detail by Mason [14]. This apparatus can be conveniently broken down into three functional parts. The first part consists of sample tube system with its heating and cooling system. The second part consists of the alignment components and the drive system. The third part consists of the satellite systems, such as the vacuum system and atmosphere control system. Figure 3 shows the schematic diagram of the main elements of first and second parts. Figure 4 shows the vacuum and inert gas system of the third part.

The sample tube is clamped between the top sample assembly and the bottom support base which are fixed to the frame and remain stationary. The furnace and cooling chamber surrounding the sample tube are attached to the drive plate which can move upward or downward at a desired velocity causing a directional solidification of the sample. A schematic diagram of the sample tube, heat assemblies and cooling chamber is shown in Figure 5.

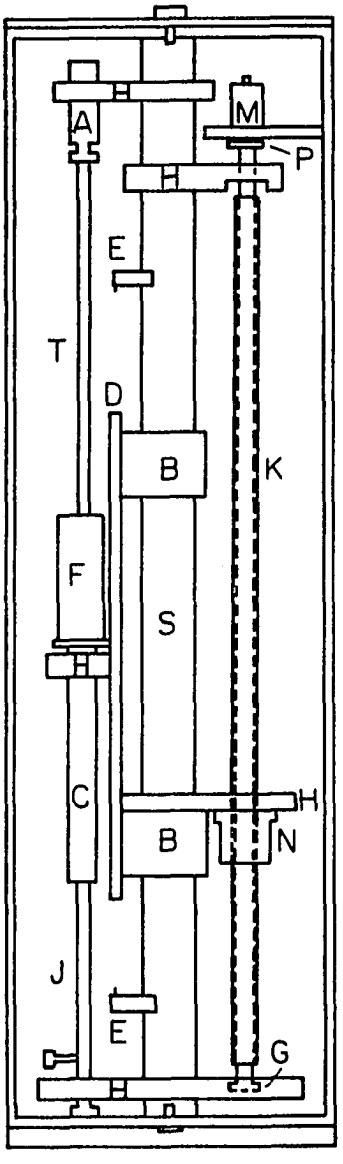

A Top sample assembly
B Square support base
C Cooling Chamber
D Drive plate
E Limiting switch
F Furnace
G Ball bearing support
H Clamp
J Bottom support base
K Ball bearing screws
M Stepping motor
N Ball bearing nut & flange
P Timer belt pulley
S Square shaft
T Sample tube

Figure 3. The main elements of directional solidification apparatus

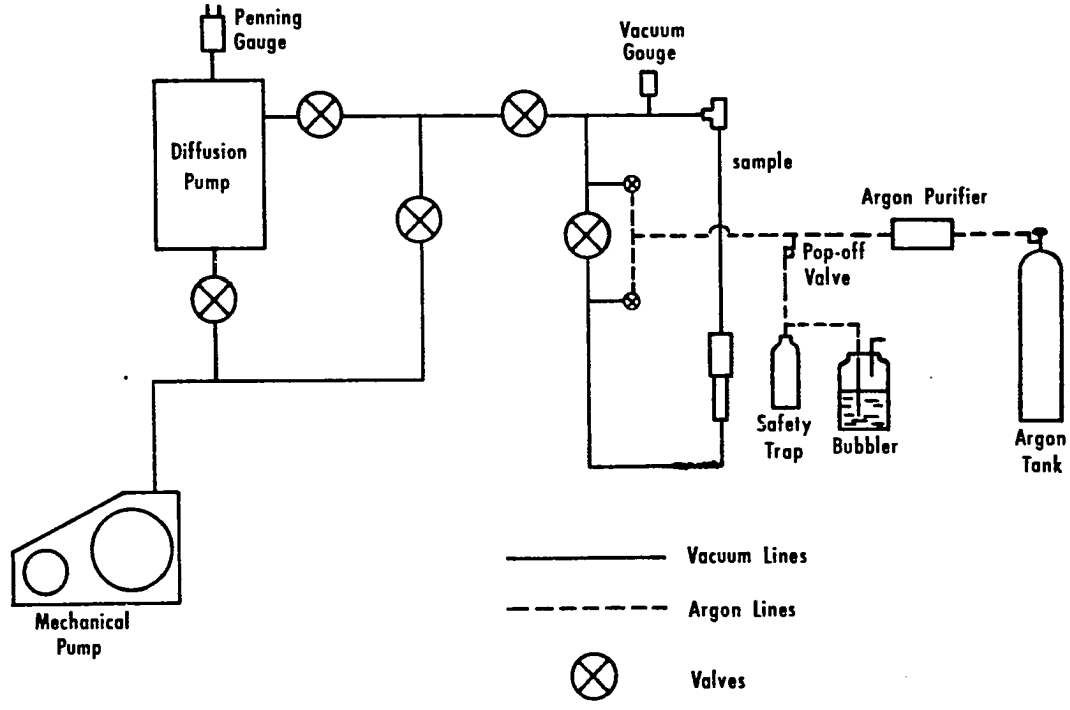

Figure 4. Vacuum and inert gas systems

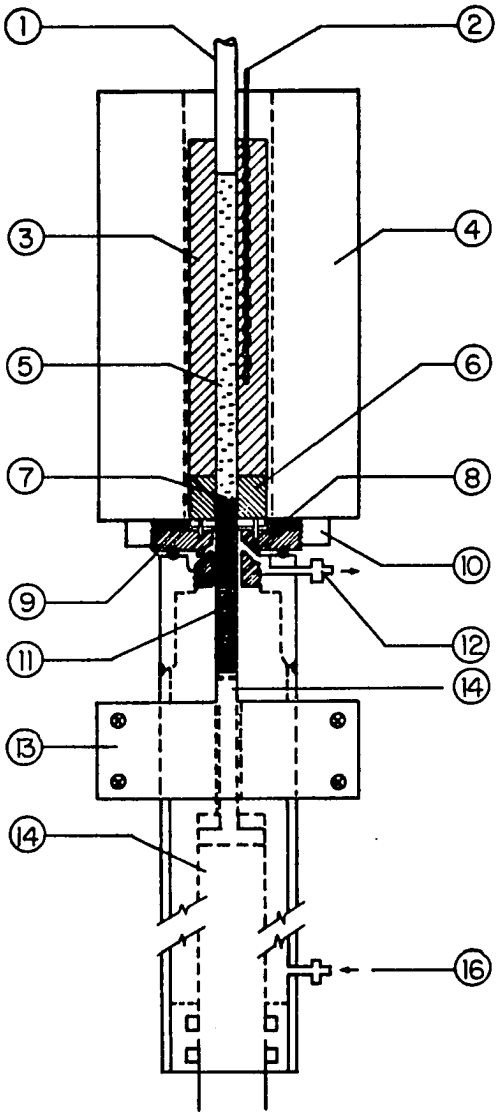

1. Sample tube
2. Thermocouple
3. Heat sink
4. Furnace
5. Sample (liquid)
6. Lava insulator
7. Solid - liquid interface
8. Graphite felt
9. Sealing flange
10. Furnace support ring
11. Sample (solid)
12. Water out
13. Clamp
14. Pedestal
15. Bottom support base
16. Water in

Figure 5. The sample tube, heater assemblies and cooling chamber

Temperature Gradient Control

In the unidirectional solidification experiments, the temperature gradients in the liquid were controlled by the furnace temperature. The temperature of the resistance furnace was controlled by a solid state time proportioning temperature controller. The sensing element was a ceramic sheathed chromel-alumel thermocouple inserted in the heat sink block.

The temperature gradient was measured by a sample thermocouple. The sample thermocouple was made from 0.004 mil wires insulated by magnesium oxide and sheathed in 0.003 mil thick, 20 mil O.D. stainless steel. The sheathed wires were supplied by Omega Engineering, Inc. The couple was made by removing the insulation material for approximately 1/16 inch from the end. This was done by alternately squeezing the end of the sheath with a flat pair of needle-nosed pliers and then agitating in an acetone wash in an ultrasonic cleaner. The sheath was then clamped in a small jig and heliarced in an inert atmosphere to melt the sheath and wires together to form a grounded lead at the end of the sheath. Approximately one-half inch of the thermocouple wires at the other end of the sheath was exposed by stripping off the stainless steel and insulation using the stripping tool. The stripped wires were connected to the male end of a subminiature thermocouple connector. The thermocouple was then encased in 0.06 inch O.D. alumina tubing which was encased in an 0.125 inch O.D. Ta tube. The alumina and Ta tubes were used to give some rigidity to the thermocouple assembly. This thermocouple was calibrated with the melting point of pure tin.

In some experiments, two solidification passes were made during each run. The first to measure the temperature gradient of the liquid at the advancing interface, and the second to obtain the desired solidification run to examine the microstructure. Initially, sufficient time was allowed for the furnace and sample to come to thermal equilibrium at the desired temperature. The sample thermocouple was inserted into the system through the access adapter. The top thermocouple connector was plugged into leads of the digital thermometer. With the drive motor on and the system at steady-state, the thermocouple was lowered into the sample to a point above the interface region such that the interface would pass through the junction of the thermocouple in a reasonable time. The strip chart was used for recording the temperature from above the liquidus to below the peritectic temperature so that the temperature gradient, at any point in this region, could be determined. After the first run, the sample was stirred to homogenize the alloy. After stirring, the sample was allowed to come to thermal equilibrium prior to starting the second solidification pass.

For convenience and to save time, we carried out experiments by controlling the furnace temperature instead of measuring the temperature gradient for each run. Therefore, we initially calibrated the sample temperature gradient as a function of furnace temperature for different growth velocities and alloy compositions. The furnace was maintained at one of the following temperatures: 300, 450, 650, 750 or 900^{o}C. The growth rates varied from 1 μm/s to 200 μm/s. The

effect of different furnace temperature on the temperature gradient in liquid at the advancing interface was first investigated for different alloy compositions. The relationship between the temperature gradients and furnace temperature was found to be linear for all peritectic alloys in the Pb-Bi system, as shown in Figure 6. The temperature gradient was also found to be affected by the growth rate for a given furnace temperature, as shown in Figure 7. These calibrated data are summarized in Table 1.

Growth Rate Control

The growth velocity of the liquid-solid interface was controlled by the drive mechanism which moved the furnace and cooling chamber at a desired rate. A timing belt pulley was attached to the top journal to transmit the stepping motor movement to the screw (see Figure 3). The motion of the screw was transmitted to the cooling chamber and furnace through the drive plate. The control unit for the stepping motor was a Commodore PET 2001 computer interfaced to the compumotor driver. The rate of travel of the drive plate was first calibrated by using a timer and dial indicator. The rates measured were used to determine the calibration adjustment factor in the drive control program for the computer. One of the calibrated test data for the growth velocities is shown in Table 2.

Microstructural Observations

Samples were directionally solidified for 6 cm length before the interface was quenched. Preparation of the samples for examination

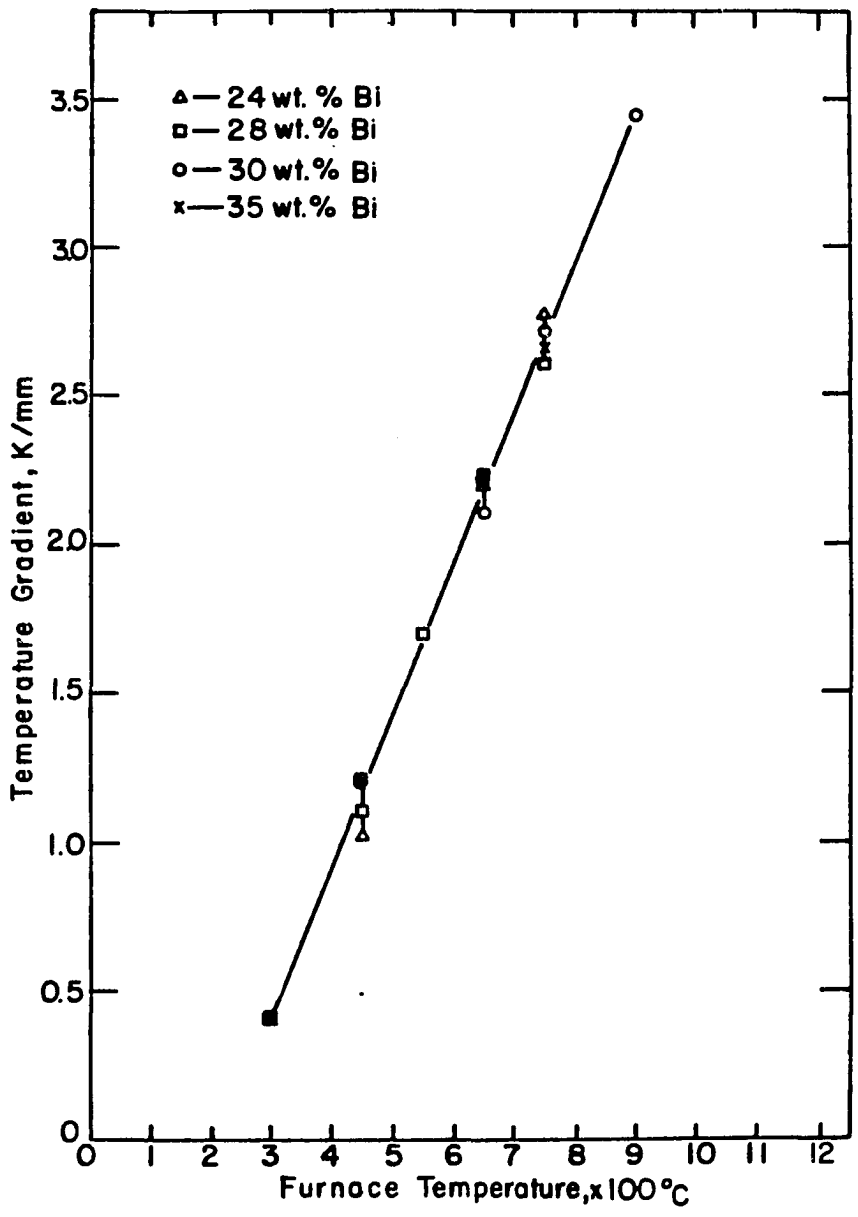

Figure 6. The calibrate curve for temperature gradient versus furnace temperature with a series of alloy compositions

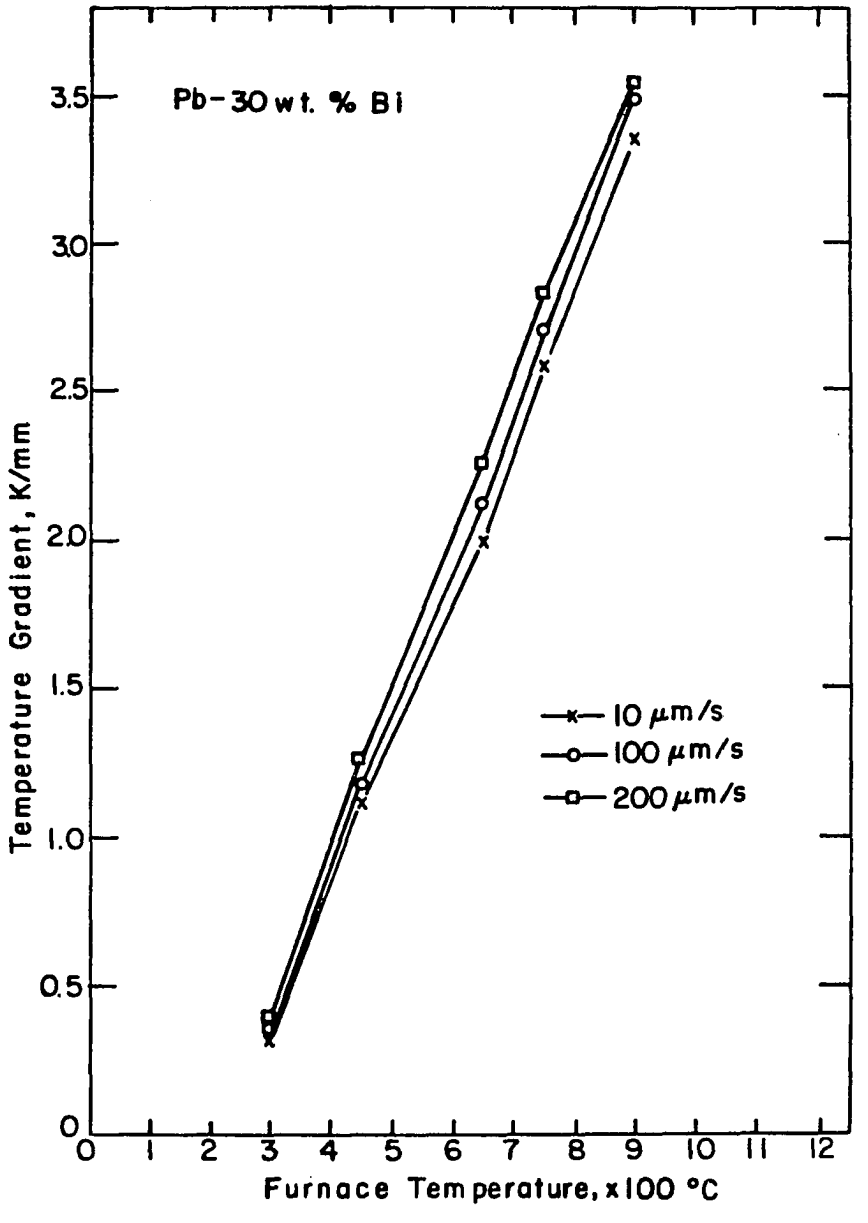

Figure 7. The effect of growth rates on temperature gradient versus furnace temperature for Pb-30 wt.% Bi alloys

Table 1. Summary of temperature gradients with respect to furnace temperature for Pb-Bi system

C (wt.% Bi)	T_f[a] (°C)	V (μm/s)	G (K/mm)
24	450	10	9.1
24	450	50	10.1
24	450	100	10.3
24	450	200	11.4
24	650	1	20.8
24	650	50	21.2
24	650	100	21.9
24	650	200	23.9
24	750	25	26.6
24	750	50	27.7
24	750	100	28.5
24	750	200	29.0
28	300	10	3.2
28	300	50	3.6
28	300	100	3.9
28	300	200	4.4
28	450	10	10.2
28	450	50	11.4
28	450	100	11.6
28	450	200	11.8
28	650	10	20.6
28	650	50	21.4
28	650	100	22.3
28	650	200	23.9
28	750	1	24.6
28	750	10	25.0
28	750	50	25.5
28	750	100	26.8
28	750	200	27.2
30	300	10	3.2
30	300	100	3.6
30	300	200	3.9
30	450	1	11.0
30	450	10	11.2
30	450	50	11.9
30	450	100	12.1
30	450	200	12.3

[a] T_f = furnace temperature.

Table 1. Continued

C (wt.% Bi)	T_f[a] (°C)	V (μm/s)	G (K/mm)
30	650	10	19.3
30	650	25	19.5
30	650	50	19.9
30	650	200	22.6
30	750	10	25.8
30	750	25	25.8
30	750	50	26.4
30	750	200	28.3
30	900	10	33.4
30	900	25	34.4
30	900	50	34.7
30	900	100	34.9
30	900	200	35.3
35	450	1	10.8
35	450	25	11.0
35	450	50	11.4
35	450	100	12.3
35	450	200	13.3
35	550	10	15.9
35	550	25	16.2
35	550	50	16.2
35	550	100	17.2
35	550	200	18.0
35	650	3	20.9
35	650	10	21.7
35	650	15	21.9
35	650	100	22.8
35	650	200	24.6
35	750	1	24.9
35	750	25	25.4
35	750	50	25.9
35	750	100	26.9
35	750	200	28.6

Table 2. Growth rate calibration

Computer program setting (μm/s)	Moving distance (mm)	Growth time (min)	Growth rate (μm/s)
0.5	4.62	155.93	0.494
1	3.20	53.34	1.000
5	4.95	16.67	4.952
10	4.32	7.27	9.900
50	25.40	8.47	49.980
100	25.40	4.23	100.079
200	50.80	4.21	201.108

began by carefully breaking the sample tube from the solidified specimen. This specimen was ground carefully along the specimen axis about 1 mm deep to get a flat surface. After polishing and etching this flat surface, the quenched interface was examined under the microscope and a mark was made at the quenched interface. Two samples for examination were obtained by sectioning the specimen with a saw. One sample was 2.5 cm long containing the quench interface position. The other sample was 1 cm long and positioned directly below the quench interface on the rod. The end closest to the quench interface sample was polished on a 600 grit silicon carbide wheel with the aid of a small fixture to obtain a surface normal to the growth direction. Both samples were then mounted in self-setting acrylic resin. The quench interface sample

positioned longitudinally along the bottom of its mount, and the second sample placed on its polished end such that the growth axis was normal to the flat bottom of the mount. The quench interface sample was then ground carefully 1~2 mm deep with 180 grit and polished through 600 grit silicon carbide. The transversely mounted sample was polished with 600 grit, keeping the plane of the polish perpendicular to the growth direction. Both samples were then micropolished with 0.3 μm alpha alumina powder on the micropolish cloth wheel. For cellular structures, the transverse section was first prepared just ahead of the interface and then the sample was ground carefully, keeping the plane perpendicular to the growth direction until the tips of the cells could be seen. These samples, after the micropolish, were etched in methanol (100 ml) + nitric acid (1-5 ml) solution to reveal the microstructure. Micrographs were taken using a camera attached to a Zeiss microscope.

EXPERIMENTAL RESULTS

Critical experiments were carried out to examine the $\alpha \rightarrow \beta$ phase transition at low growth rate and at high growth rate for Pb-30 wt.% Bi and Pb-35 wt.% Bi alloys, respectively. In order to study the condition at which a planar α:β interface exists, the variation in the length (ℓ) of α dendrite or cell ahead of the β-phase was studied as a function of growth rate (V), temperature gradient (G) and alloy composition (C). Critical experimental conditions were determined for which $\ell \rightarrow 0$. The tip temperatures at α-phase and β-phase were also measured for Pb-30 wt.% Bi at G = 21.5 K/m for different velocities to determine the interface temperature when $\ell \rightarrow 0$. In these experiments, the specimen for the solidification run was about 10.5 cm long and 6 mm O.D. The growth length before quench was 6 cm in each run.

$\alpha \rightarrow \beta$ Phase Transition at Low Velocity

The effect of low growth rate on the $\alpha \rightarrow \beta$ phase transition is shown in Figure 8 for the Pb-30 wt.% Bi alloys directionally solidified at G = 21.5 K/mm and at velocities ranging from 0.75 μm/s to 2.5 μm/s. At V = 2.5 μm/s, the α-phase dendrite solidifies ahead of the nonplanar β-phase, as shown in Figure 8a. As V decreases (V = 1.5 μm/s), the α-phase change from dendrite to cells, and the cellular front still grows ahead of the β-phase, although the length, ℓ, between the α-phase tip to the β-phase front decreases (Figure 8b). As V is decreased, a critical velocity is obtained at which the value of ℓ approaches zero,

Figure 8. Longitudinal photographs of Pb-30 wt.% Bi alloys at G = 21.5 K/mm with V = (μm/s): a) 2.5, b) 1.5, c) 1.0, and d) 0.75

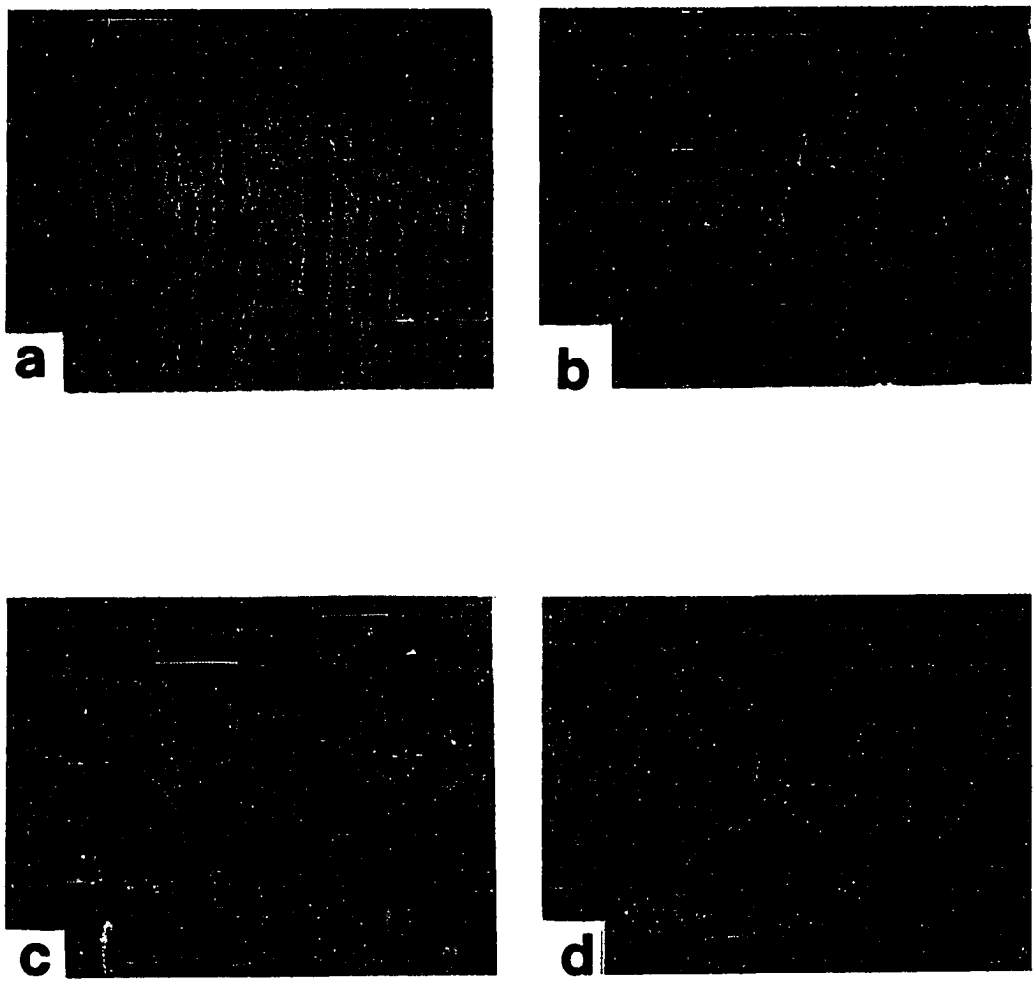
a
b
c
d

i.e. the α-phase and β-phase grow at the same front, and the solidification structure is found to form by the cooperatuve growth of α and β phases, as shown in Figure 8c. When V is smaller than the critical value, the solid-liquid interface is planar and the β phase is formed as shown in Figure 8d.

α-dendrite to β-dendrite Transition at High Velocity

In this experiment, α-dendrite to β-dendrite transition is studied for Pb-35 wt.% Bi alloys. Figure 9 shows the changes in interface morphology with growth rate at G = 22 $\pm$ 1.0 K/mm. At V = 50 μm/s, the transverse section of the sample shows the α-dendrite structure at the top. At V = 100 μm/s, the transverse section just behind the tip exhibits a mixed structure which coexists of α-dendrites and β-dendrites. At higher growth rate, V = 500 μm/s, only β dendrite is found on the micrographs of the transverse section. These observations confirm the theoretical prediction of α to β phase under both growth rate conditions.

Dendrite and Cell Length

The variation of the length (ℓ) of dendrite or cell ahead of the β-phase with growth rate is studied for several alloys near the peritectic compositions at a series constant temperature gradient values. Our aim was to extrapolate the length to zero to obtain the growth rate value at which α and β phases could be grown cooperatively.

The variation in ℓ was studied as a function of growth rate, temperature gradient and composition. Figure 10 shows the effect of

Figure 9. The morphology of α-dendrite and β-dendrite transition for Pb-35 wt.% Bi alloys at G = 22 ± 1.0 K/mm with V = (μm/s): a) 50, b) 100, and c) 500. M = 28.54x (a); M = 78.6x (b, c)

(a)

(b)

(c)

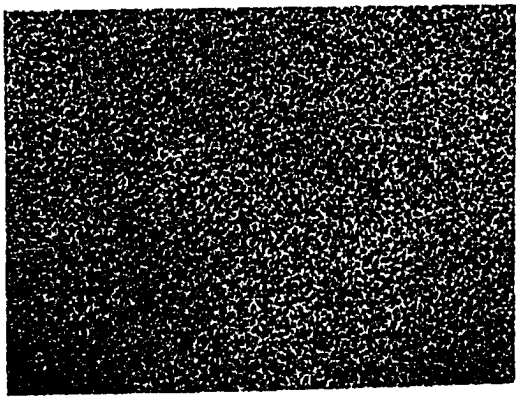

growth rate and temperature gradient for Pb-30 wt.% Bi alloys. For a constant temperature gradient condition, a linear relationship was found between ℓ and V, if the α-phase grew as a dendrite. However, if the α-phase formed a cellular structure, then the value of ℓ was found to decrease sharply with decreasing velocity until the value of ℓ equaled zero, at which point both the α and β phases grew with the same interface front.

The effect of temperature gradient on ℓ can be seen in Figure 10 which shows that ℓ is increased as G is decreased. This variation of ℓ with G is shown in Figure 11. For dendritic structures, a linear relationship between ln ℓ and ln G was found for a series of constant velocities. However, a sharp decrease in ℓ with G is observed for cell structures. For $V > 3$ μm/s, the temperature gradient values required for $\ell = 0$ were much higher than those which could be obtained experimentally. However, the basic nature of the plot, exhibited by the 1.5 μm/s data, should be observed for higher velocity values under higher temperature gradient conditions. The values of the critical velocity, V_{cr}, at which $\ell \rightarrow 0$ were obtained from Figures 10 and 11. The variation in V_{cr} with G is plotted in Figure 12 for Pb-30 wt.% Bi. This plot is the locus of points for which a cooperative growth of $\alpha \rightarrow \beta$ phase will occur in the Pb-30 wt.% alloy.

The effect of alloy composition on ℓ is shown in Figure 13. The dendrite or cell length is found to decrease as the composition is increased for constant V and G conditions. These results are plotted in Figure 14 which show a linear variation in ℓ vs. C when a dendritic

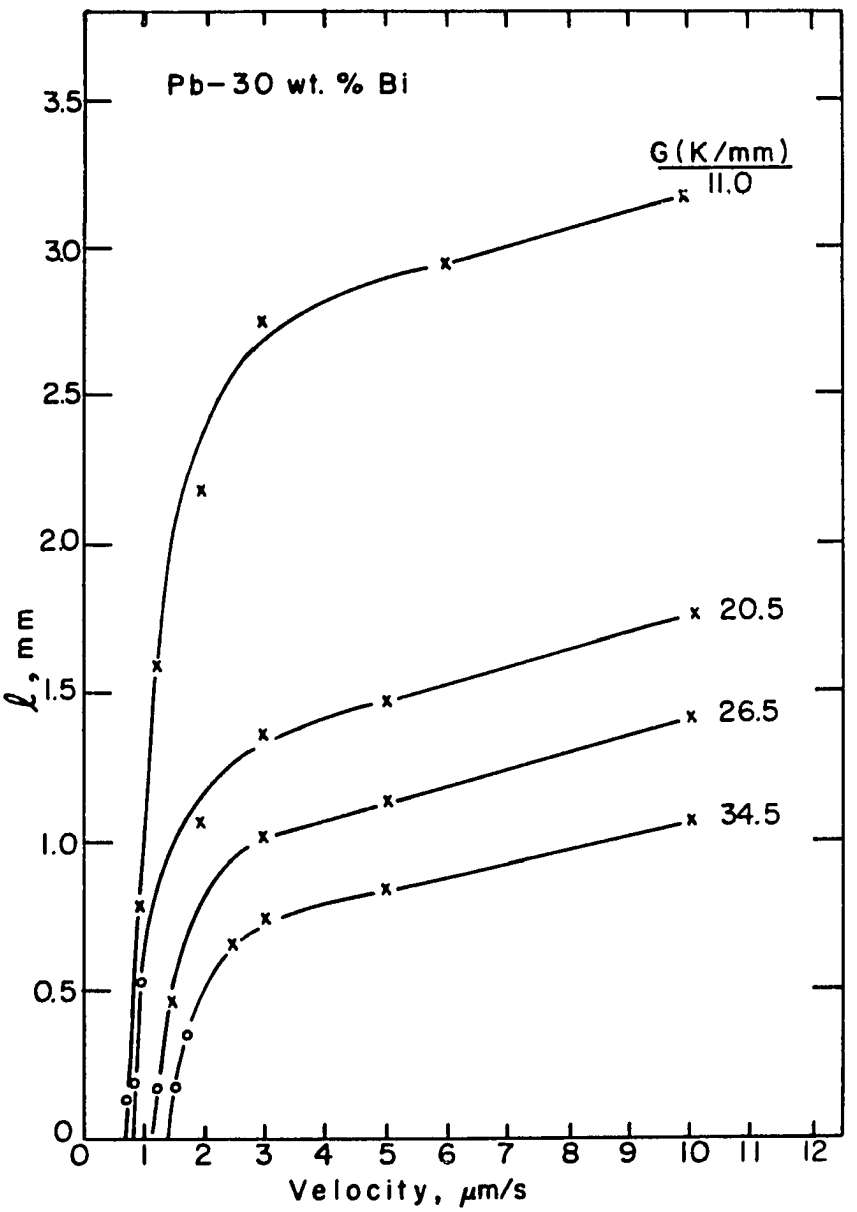

Figure 10. Variation in α-phase length (ℓ) ahead the β-phase with growth rates of Pb-30 wt.% Bi at a series of temperature gradient values

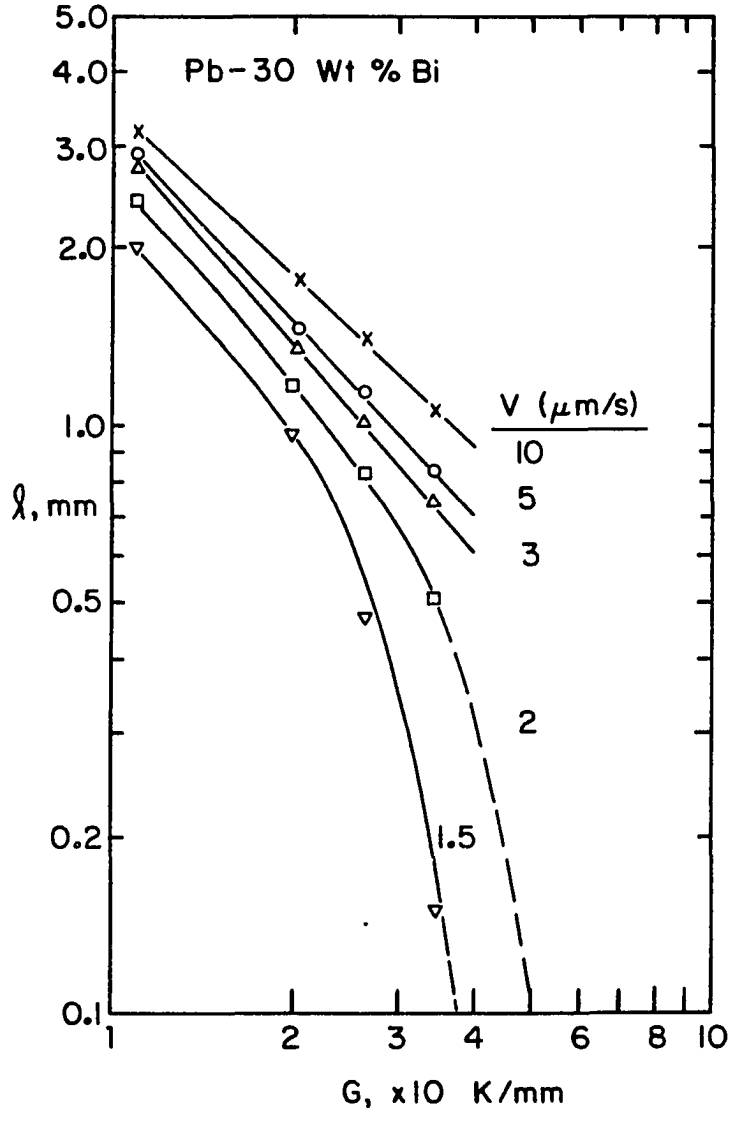

Figure 11. Variation in ℓ with G for Pb-30 wt.% Bi at a series of growth rate values

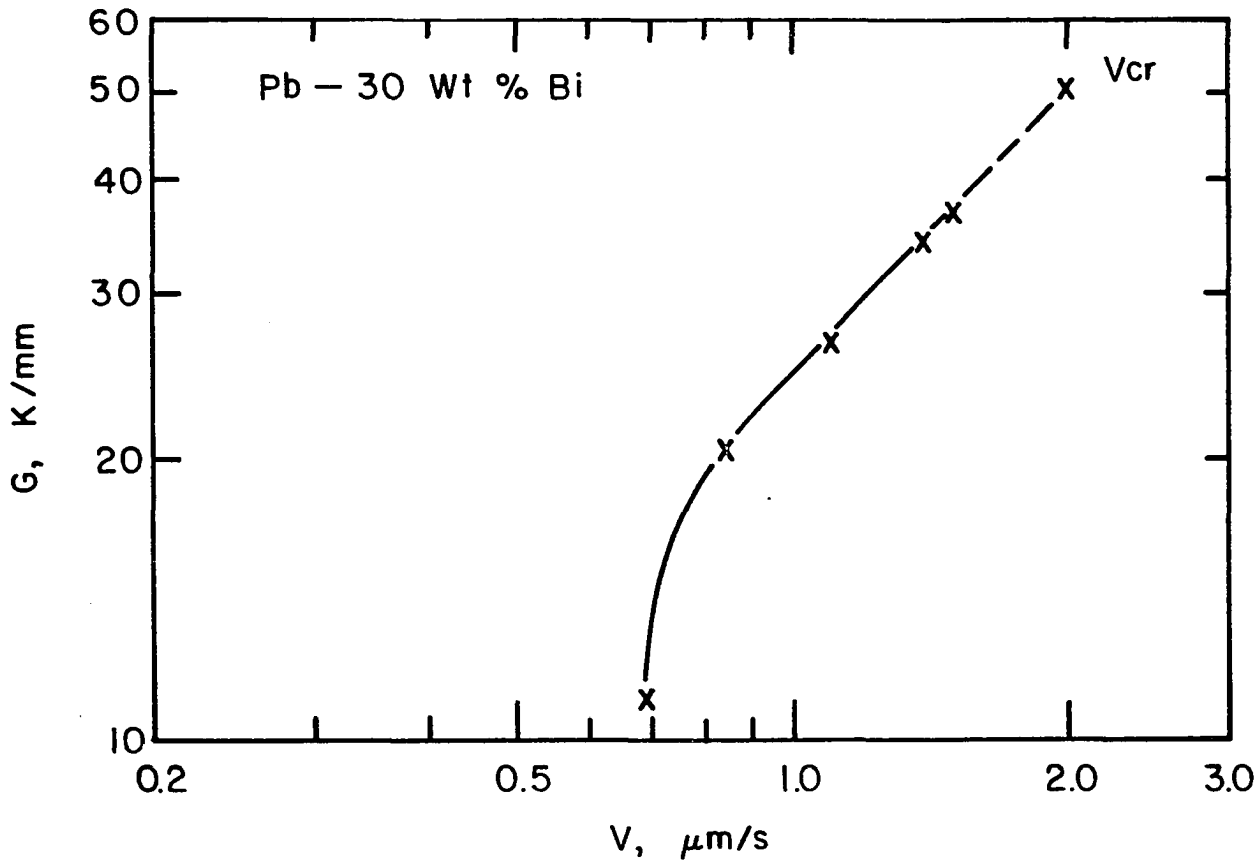

Figure 12. G versus V_{cr} data for Pb-30 wt.% Bi at fs = 0.57

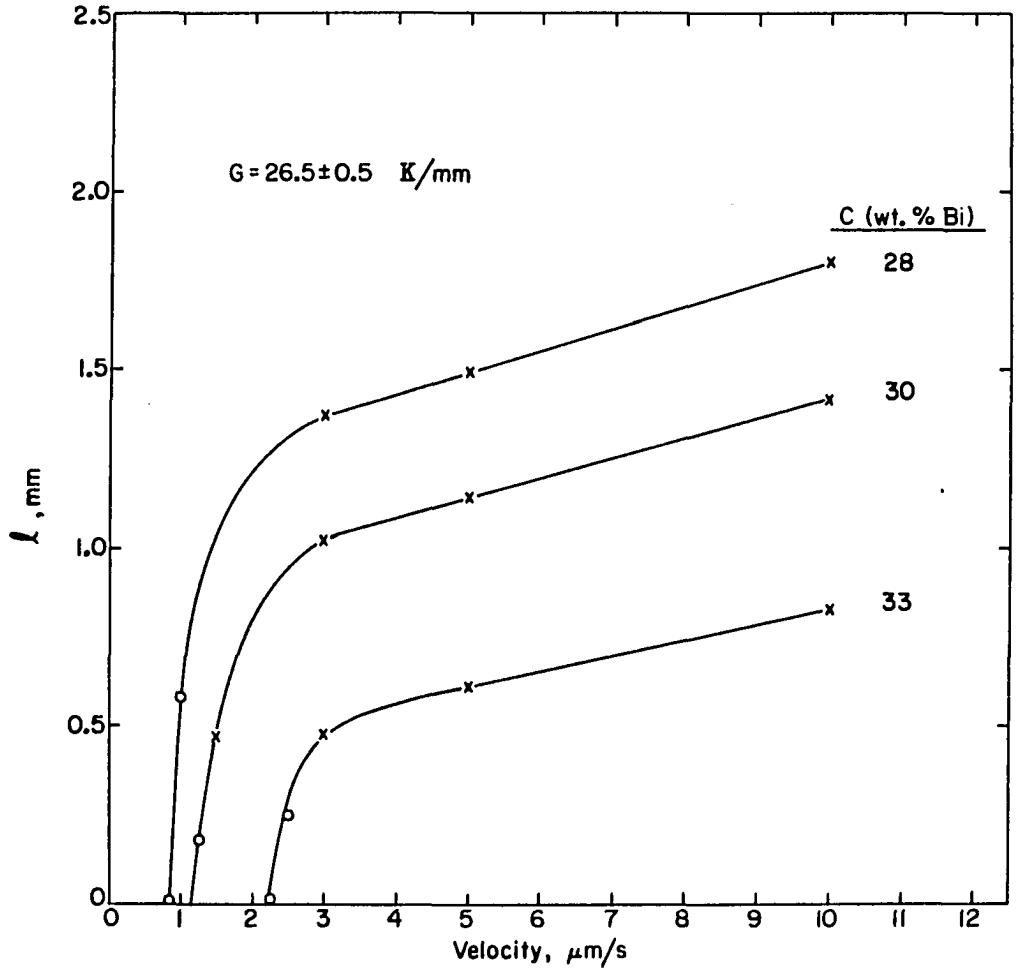

Figure 13. Variation in ℓ with growth rate for a series of alloy compositions at G = 26.5 K/mm

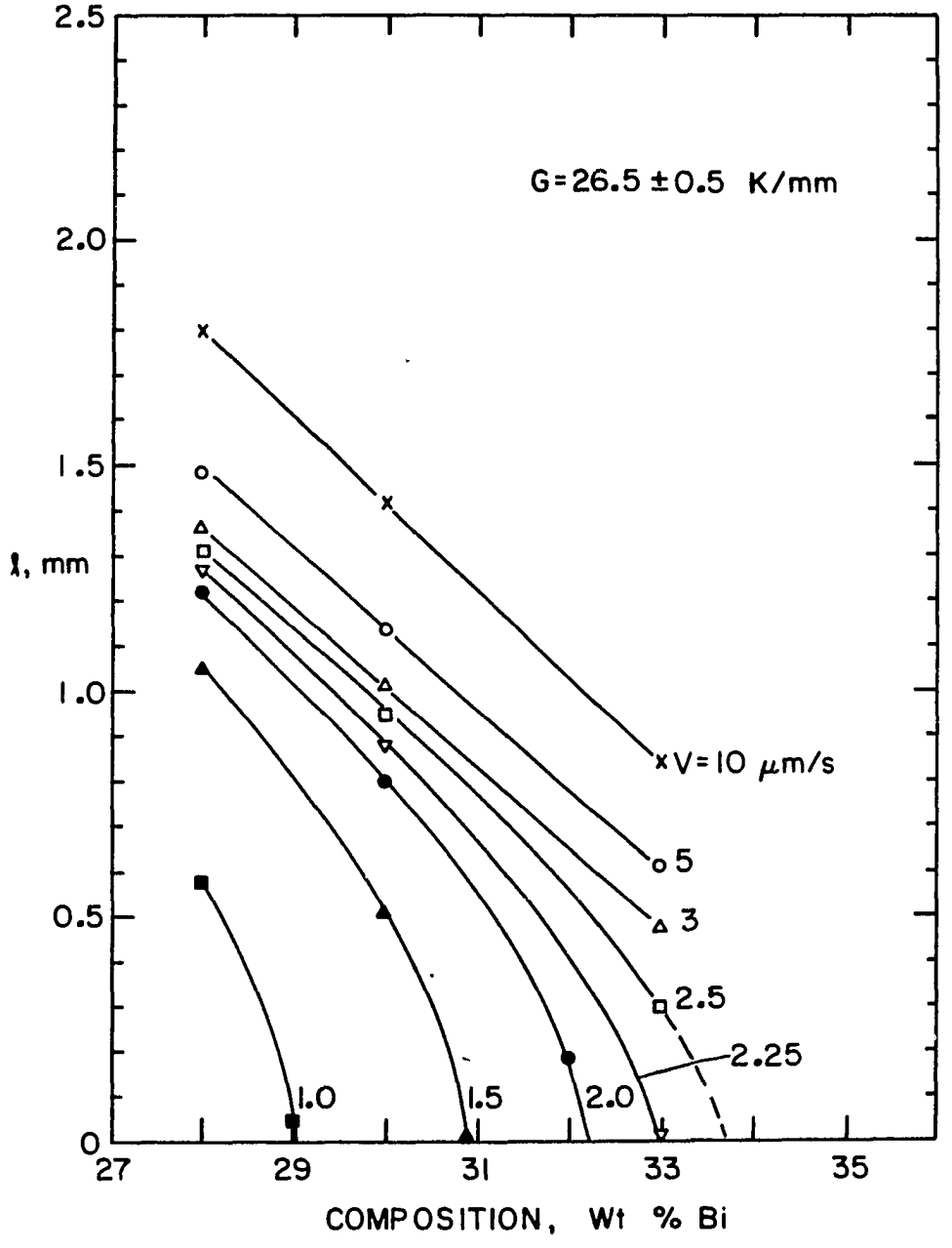

Figure 14. Variation in ℓ with alloy compositions at G = 26.5 K/mm and a series growth velocity values

structure is present. However, a sharp departure from linearity is observed when cellular structures form. Figure 15 shows the variation of V_{cr} as a function of composition for G = 26.5 K/mm. A linear relationship is observed between ln V_{cr} and ln C. Thus, we may write $V_{cr} \alpha C^{n}$, where n = 6.27. The experimental data for the dendrite and cell length are given in Tables 3 and 4.

Temperatures at α-phase and β-phase Fronts

The interface temperatures for α phase and β phase were measured in the Pb-30 wt.% Bi alloys at G = 21.5 K/mm for a series of velocities. In these experiments, the thermocouples were first calibrated and then placed in the directional solidification equipment at a distance of about 0.5 cm from the interface. The thermocouple was left in the sample and the directional solidification run carried out until the interface passed the thermocouple. The sample, with the thermocouple in it, was then quenched, and a longitudinal section was prepared which showed the position of the thermocouple bead. Figure 16 shows the thermocouple embedded in the sample of Pb-30 at.% Bi which was directionally solidified at V = 1 μm/s and G = 21.4 K/mm. The distance between the thermocouple bead and the α and β front was measured from the micrographs and the temperatures of α and β fronts were calculated from the thermocouple trace at these distances. The thermocouple calibration results are given in Table 5, and the interface temperatures are listed in Table 6. The variation in α and β front temperature with velocity is shown in Figure 17.

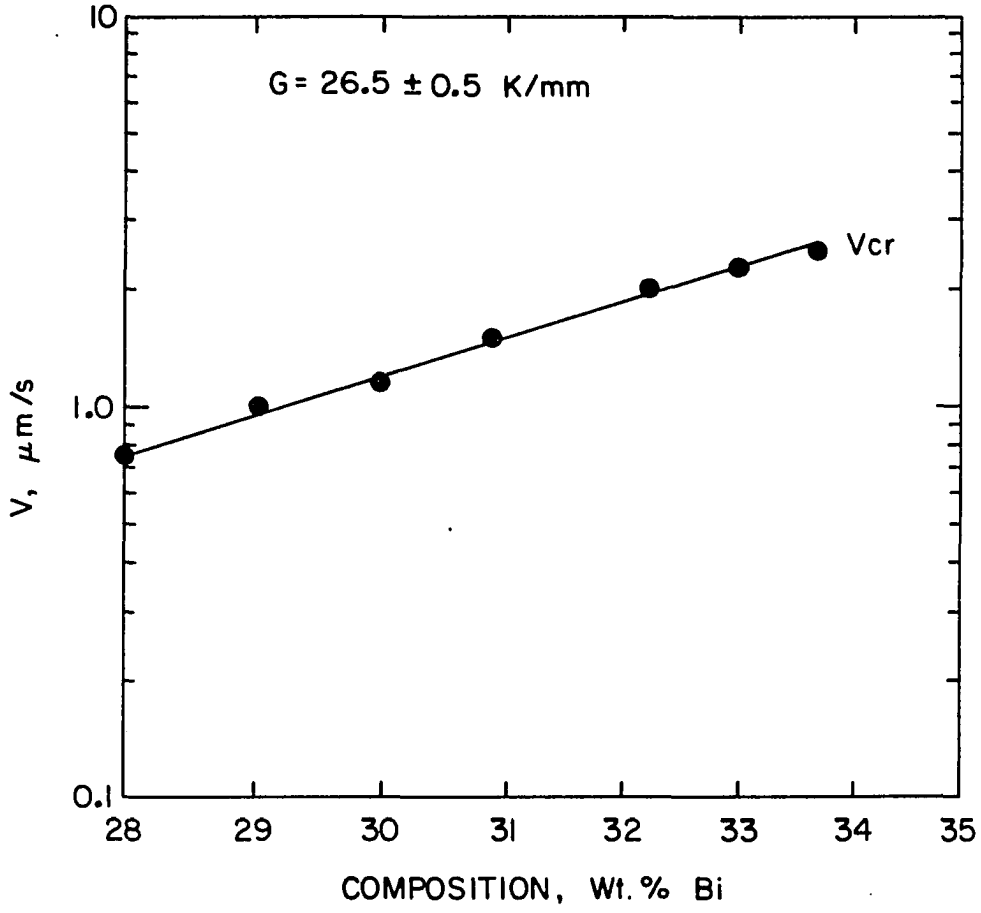

Figure 15. V_{cr} versus alloy composition data at G = 26.5 K/mm and fs = 0.57 conditions (composition in log scale)

Table 3. The length of α-phase ahead the β-phase (sample length = 10.5 cm; growth length = 6 cm)

C (wt.% Bi)	G (K/mm)	V (μm/s)	ℓ (mm)	Microstructure[a] morphology	
28	26.5	10	1.80	α:D	β:N
		5	1.49	α:D	β:N
28	26.5	3	1.37	α:D	β:N
		1	0.58	α:C	β:P
		0.8	~0.02	α:C	β:P
		10	3.18	α:D	β:N
		6	2.95	α:D	β:N
		3	2.75	α:D	β:N
30	11.0	2	2.20	α:D+C	β:N
		1.25	1.60	α:D+C	β:P
		1.0	0.79	α:C+D	β:P
		0.75	0.14	α:C	β:P
		10	1.76	α:D	β:N
		5	1.47	α:D	β:N
		3	1.35	α:D	β:N
30	20.5	2	1.07	α:D+C	β:N
		1	0.54	α:C	β:P
		0.9	0.19	α:C	β:P
		10	1.42	α:D	β:N
		5	1.14	α:D	β:N
30	26.5	3	1.02	α:D	β:N
		1.5	0.47	α:D+C	β:P
		1.25	0.18	α:C	β:P
		10	1.07	α:D	β:N
		5	0.84	α:D	β:N
		3	0.74	α:D	β:N
30	34.5	2.5	0.66	α:D+C	β:N
		1.75	0.35	α:C+D	β:P
		1.50	0.18	α:C	β:P

[a]D = dendrite, C = cell, P = planar interface, and N = nonplanar interface.

Table 3. Continued

C (wt.% Bi)	G (K/mm)	V (μm/s)	ℓ (mm)	Microstructure[a] morphology	
		10	0.84	α:D	β:N
		5	0.61	α:D	β:N
33	26.5	3	0.48	α:D	β:N
		2.5	0.25	α:C	β:P
		2.25	~0.02	α:C	β:P
29	26.5	1	0.1	α:C	β:P
31	26.5	1.5	--	α:P	--
32	26.5	2.0	0.43	α:C+D	β:N(C)
34	26.5	2.5	--	α:C	β:C

Table 4. Critical growth rate for α-β transition (sample length = 10.5 cm; growth length = 6 cm)

C (wt.% Bi)	G (K/mm)	V_{cr} (μm/s)	G/V_{cr} (x 10^{-2} K-s/μm^2)
28	26.5	0.80	3.31
29.05	26.5	1.0	2.65
30	11.0	0.70	1.57
30	20.5	0.85	2.41
30	26.5	1.10	2.41
30	34.5	1.40	2.46
39.0	26.5	1.50	1.77
32.2	26.5	2.00	1.38
33	26.5	2.25	1.18
33.7	26.5	2.50	1.06

Figure 16. The distance measured between sample thermocouple conjunction and α- and β-phase front from longitudinal section of specimen after run. (Pb-30 wt.% Bi alloy under G = 21.5 K/mm and V = 1 μm/s conditions)

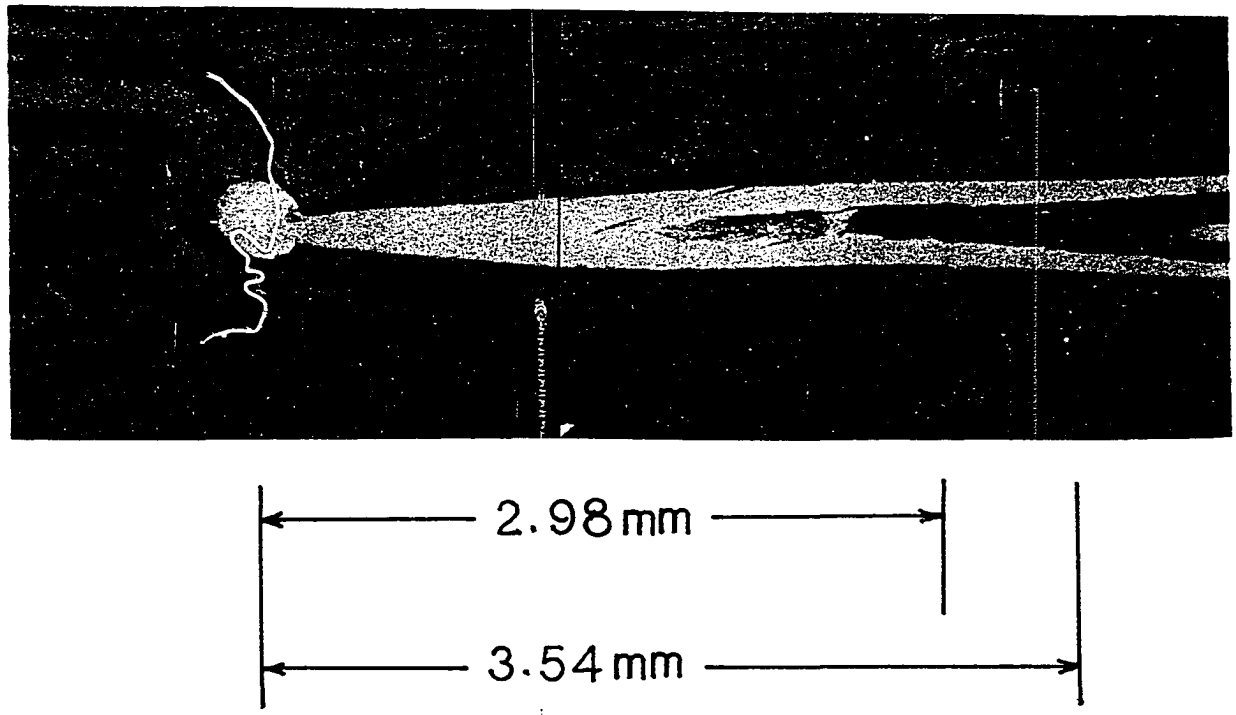
2.98mm
3.54mm

Table 5. Sample thermocouple calibration data[a]

Thermocouple number	T_m (measure) (°C)	Reading error[b] (°C)
1	234.57	2.59
2	235.12	3.14
3	234.20	2.22
4	237.18	5.20
5	236.17	4.19
6	237.48	5.50

[a]5'9s pure tin.

[b]Calculate with pure tin melting point (T_m = 231.98°C.

Table 6. Tip temperature experimental data (Pb-30 wt.% Bi)

V (μm/s)	G_ℓ [a] (K/mm)	G_s [a] (K/mm)	ℓ_α [b] (mm)	ℓ_β [b] (mm)	α-front temp. (°C)	β-front temp. (°C)	T.C. #1
0.9	21.8	16.9	1.77	1.49	192.8	187.83	4
1.0	21.4	16.2	3.54	2.98	194.7	184.8	1
2.0	19.3	11.9	5.33	4.26	215.9	197.2	2
5.0	21.2	16.3	4.91	3.44	221.8	191.4	3
10.0	21.6	16.6	4.48	2.80	221.9	188.4	5
50.0	21.1	16.9	5.26	--	220.9	--	6

[a] G_ℓ , G_s = temperature gradient in liquid and solid phase, respectively.

[b] ℓ_α, ℓ_β = distance between α-, β-phase front and the center of the thermocouple tip.

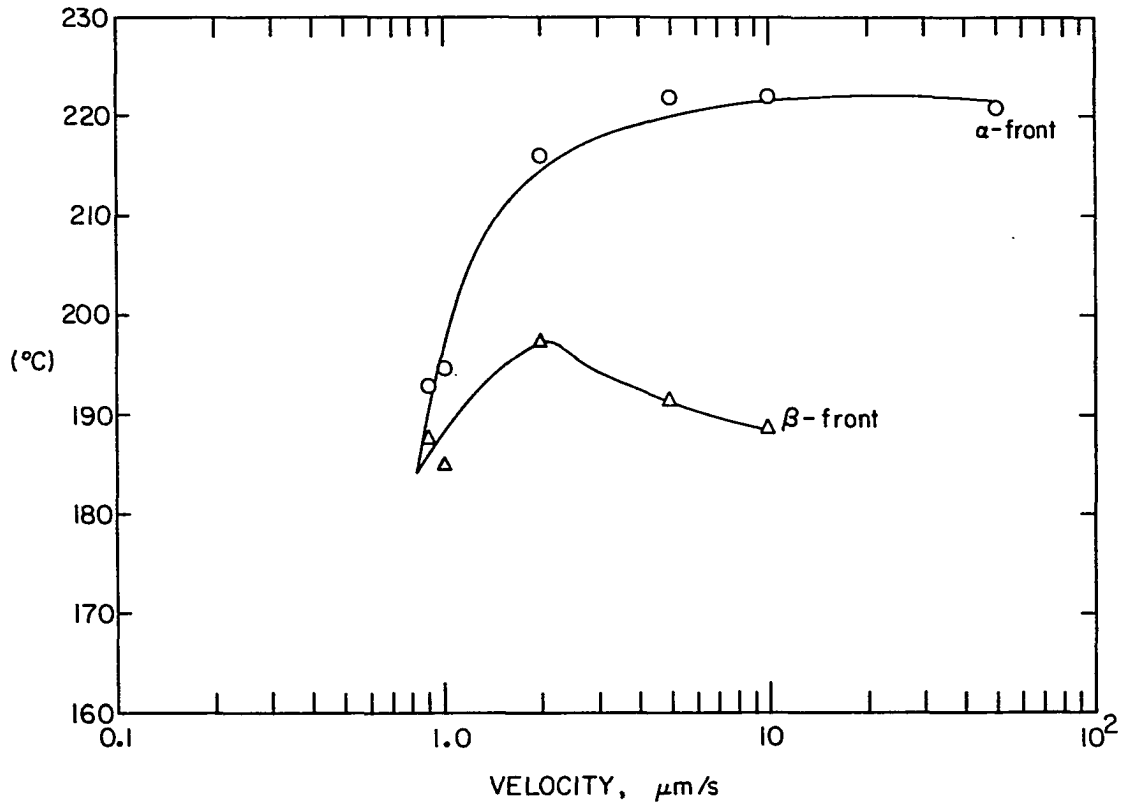

Figure 17. Front temperature of α- and β-phase versus growth rate data for Pb-30 wt.% Bi at G = 21.5 K/mm condition

DISCUSSION

Our experimental results show that the α to β phase transition occurs at low velocity as well as at high velocity. Since, at the high velocity transition, both α and β phases grow as dendrites, the theoretical model based on the isolated dendrite tip temperature would be expected to qualitatively predict this transition. Recent experimental studies by Somboonsuk and Trivedi [15] on a model transparent system have shown that the dendrite tip temperature does not couple strongly with the neighboring dendrites. Consequently, dendrite tip temperatures, calculated on the basis of noninteracting α and β tip temperatures, would give us a reasonable model to compare the relative tip temperatures. Thus, using the idea first presented by Jackson and Hunt [13], the phase that has the higher temperature will be the stable phase. Theoretical calculations, shown in Figure 2, predict the α to β transition at $V \sim 100$ μm/s in the Pb-35% Bi system at $G = 26.5$ K/mm. Our experimental results show that α dendrites are formed at $V = 50$ μm/s, whereas β dendrites form at $V = 500$ μm/s. At 100 μm/s, both α and β dendrites are found to exist. Consequently, the $\alpha \rightarrow \beta$ transition occurs at V just above 100 μm/s, a result which agrees with the theoretical model.

The low velocity transition has also been observed experimentally, and critical conditions were determined at which $\alpha \rightarrow \beta$ transition occurs. At this critical condition, both α and β phases were found to coexist and the α:β interface was found to be planar. Consequently, for a given alloy, a (V, G) condition exists at which α and β phases grow cooperatively. These critical conditions were obtained from the

measurements of dendrite or cell length and then taking the limit as $\ell \to 0$. The variation in critical velocity as a function of G at constant C, and as a function of C at constant G, was obtained. The variation in the G/V_{cr} ratio versus C is plotted in Figure 18, and a straight line relationship is obtained. Consequently, we may write the critical condition as

$$\frac{G}{V} = A - BC$$

where the values of A and B, obtained from a linear regression analysis, are: $A = 14.24$ K-s/μm^2, $B = 0.396$ K-s/μm^2 wt.%. For the Pb-Bi system, the value of $m_1/D_L \simeq 0.32$, which is close to the value of the slope B. Also, A/B is approximately equal to 36 wt.%. Consequently, the critical conditions obtained for the α to β transition are equivalent to the condition, given by Equation (3). Thus, our results are in agreement with the results of Brody and David [3] in the Pb-Bi system.

The basic theoretical ideas, presented in Figure 2, appear to be valid in that the α phase dendrites first transfer to α phase cells, and the length of the cell decreases until it becomes zero. At this point, both α and β phases grow cooperatively. Below this velocity, only β phase is found. The quantitative comparison with Figure 2 has been shown not to be valid, and this was discussed earlier to be due to strong interactions between the α and β phases which exist as $\ell \to 0$. In addition to this, our experimental results on tip temperature show a distinctly different behavior as the critical velocity is approached.

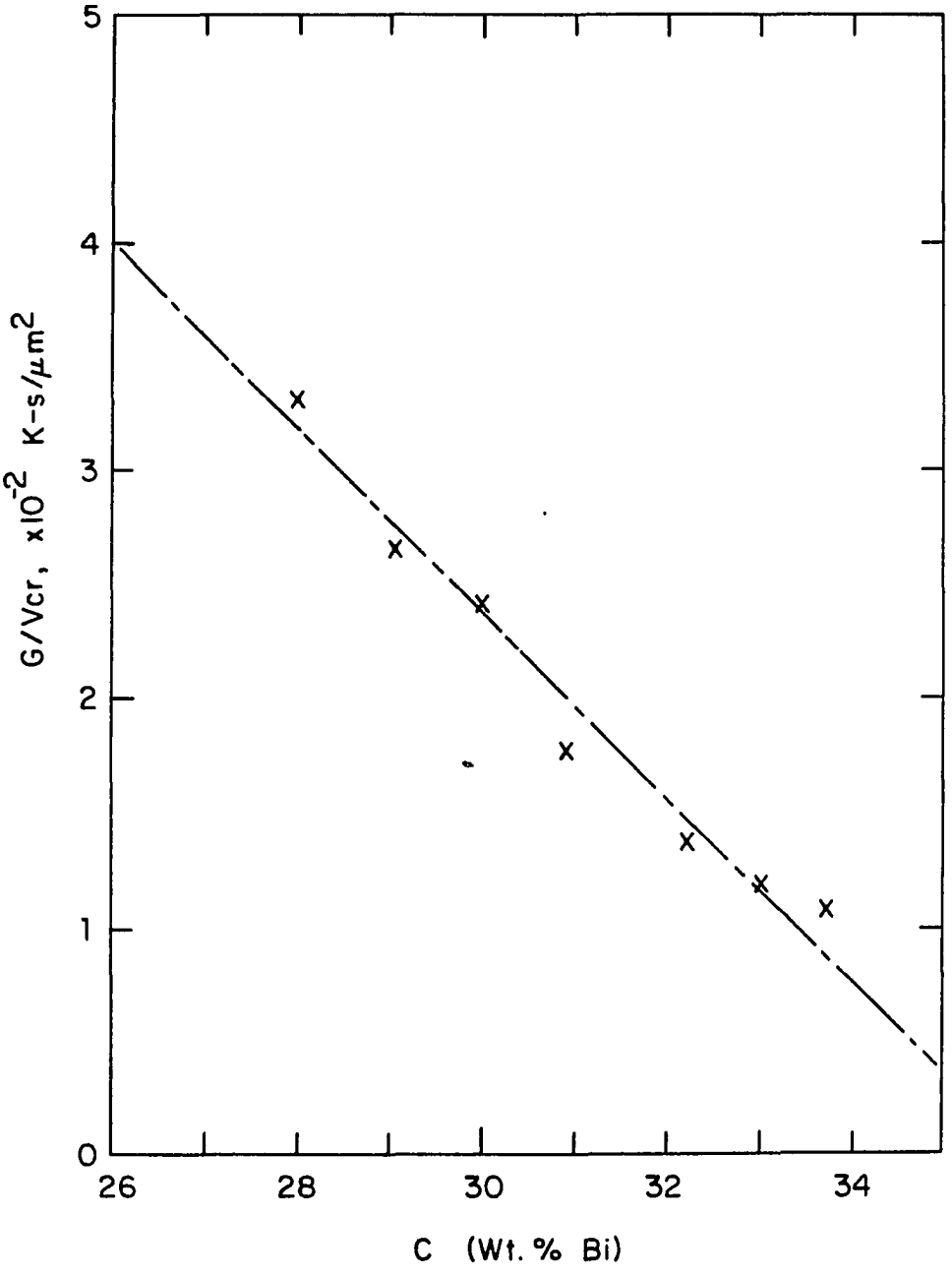

Figure 18. Critical G/V_{cr} vs. C plot for Pb-30 wt.% Bi alloys

This, we believe, is due to the presence of strong convection effects at low velocities. A number of the interesting observations on α and β interface temperatures were observed. (1) At low velocity, α and β interface temperatures become equal when both phases grow cooperatively. This temperature is found to be the peritectic temperature. (2) A local maximum in β-phase temperature with velocity is observed. A correlation of β-phase temperature with the microstructure shows that this local maximum occurs at the cell to dendrite transition in the leading α-phase morphology. (3) The interdendritic β-phase morphology is planar at V = 0.9 and 1.0 μm/s (see Figure 17). However, at V = 2-10 μm/s, it is cellular. The β-phase at V = 50 μm/s is dendritic.

As the β-phase planar interface becomes unstable, the β-phase temperature will increase as observed by the experimental results. The decrease in β-phase temperature, however, is unexpected. Two plausible explanations can be given to understand this behavior. First, the β-phase location is not fixed since the β-phase can exist over a range of temperatures or compositions. The precise selection criterion for the β-phase location could be more complex. Second, in our experiments, the solidification is carried out such that the solid grows upwards. Since Bi is lighter than lead, the liquid is unstable with respect to density driven convection. At low velocities, the convection effects become quite pronounced. Since the α - β transition velocity is smaller than 1 μm/s, a significant convection effect could be present in our system.

If strong convection effects are present, we would expect significant macrosegregation, and consequently, a change in dendrite interface characteristics with time. In order to check this point, experiments were carried out in which the fraction solidified was varied from 0.2 to 0.7, and α-dendrite lengths were measured. A systematic decrease in dendrite length was observed as the fraction solidified was increased, as shown in Figure 19. Since dendrite length is approximately given by the relationship, $\ell = \Delta T/G$, a decrease in length would correspond to the decrease in ΔT, where ΔT is the temperature difference between the α-dendrite tip and the β-phase front. Thus, our experimental results show that ΔT decreases with the fraction solidified.

In order to check the presence of macrosegregation, a chemical analysis was obtained for samples with fraction solidified as 0.3, 0.5 and 0.7. These samples were taken at a fixed distance of 1.5 mm from the α-dendrite front. The results show that the average composition at a given distance from α-dendrite tip increased slightly as the fraction solidified increases, as shown in Table 7. Consequently, the variation in β-phase temperature appears to occur due, at least in part, to the presence of convection.

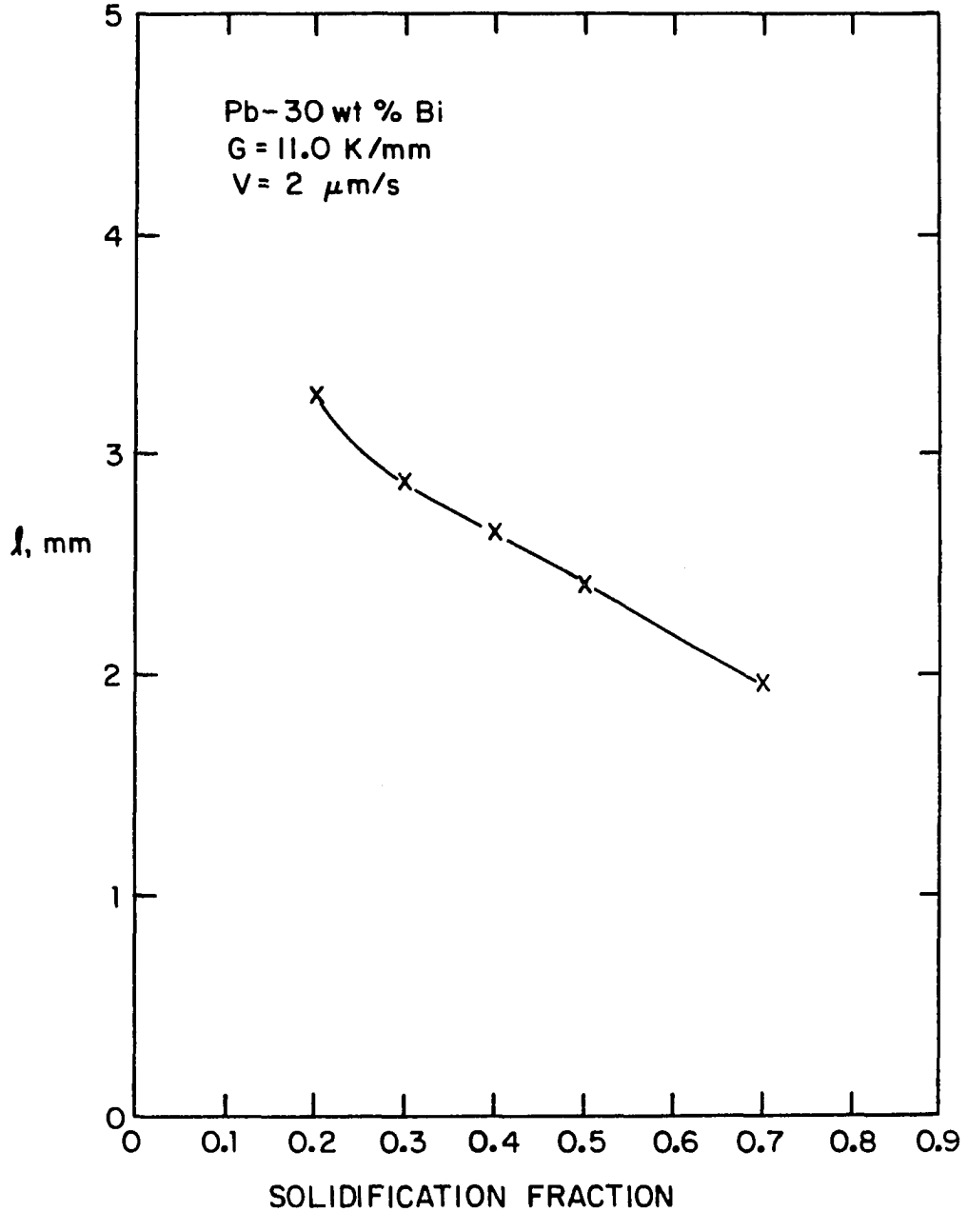

Figure 19. ℓ versus solid fraction data for Pb-30 wt.% Bi alloy at G = 11 K/mm and V = 2 μm/s conditions

Table 7. Macrosegregation analysis for Pb-30 wt.% Bi alloy under G = 11 K/mm and V = 2 μm/s conditions

fs	Wt.% Bi[a]
0.3	30.62
0.5	31.52
0.7	32.47

[a]Samples were taken at a fixed distance of 1.5 mm from the α-dendrite front.

CONCLUSIONS

(1) In the lead-bismuth peritectic alloys, the α to β phase transition has been found to occur at low growth rate, as well as at high growth rates.

(2) The critical growth rate at which the α phase and β phase grow cooperatively with a planar front has been determined experimentally. A relation of the form $(G/V) = A - BC$ has been found for fixed solidified fraction, where $A = 14.24$ and $B = 0.396$ in Pb-Bi alloys at $fs = 0.57$.

(3) For a constant temperature gradient, a linear relationship was found between ℓ and V if the α-phase grew as a dendrite. However, if the α-phase formed a cellular structure, then the value of ℓ was found to decrease sharply with decreasing velocity.

(4) At low growth rate regime, a linear relationship between $\ln \ell$ and $\ln G$ was found for a series of constant V for dendritic structure. A sharp decrease in $\ln \ell$ vs. $\ln G$ is observed for cell structures.

(5) The dendrite or cell length is found to decrease as the composition is increased for constant V and G conditions. There is a linear variation in ℓ vs. C when dendritic structure is present and a sharp departure from linearity is observed when cellular structures form.

(6) Convection effects were found to be significant near the low velocity $\alpha \rightarrow \beta$ transition point.

REFERENCES

1. Mollard, F. R. and Flemings, M. C. Trans. TMS-AIME 1967, 239, 1526-1546.

2. Rinaldi, M. D., Sharp, R. M. and Flemings, M. C. Met. Trans. 1972, 3, 3133-48.

3. Brody, H. D. and David, S. A. Int. Conf. Solidification and Casting, Sheffield, July 1977, 1, 144 pp.

4. Bower, T. F., Brody, H. D. and Flemings, M. C. Trans. Metall. Soc. AIME 1966, 236-624.

5. Burden, M. H. and Hunt, J. D. J. Cryst. Growth 1974, 22, 328.

6. Jin, I. and Purdy, G. R. J. Cryst. Growth 1974, 23, 29.

7. Kurz, W. and Fisher, D. J. Acta Met. 1981, 29, 11.

8. Trivedi, R. J. Cryst. Growth 1980, 49, 219.

9. Trivedi, R. Acta Met. 1970, 18, 287.

10. Huang, S. C. and Glicksman, M. E. Acta Met. 1981, 29, 701.

11. Chalmers, B. Physical Metallurgy. John Wiley and Sons, Inc., New York. Second printing, 1962, Chapter 6, p. 231.

12. St. John, D. H. and Hogan, I. M. J. Materials Science 1982, 17, 2413-2418.

13. Jackson, K. A. and Hunt, J. D. Trans. Metall. Soc. AIME 1967, 239, 864.

14. Mason, J. T. An Apparatus for Directional Solidification, IS-4817, UC-37, Nov. 1982.

15. Somboonsuk, K. and Trivedi, R. J. Material Science (in press).

SECTION II. PRIMARY CELL AND DENDRITE SPACING IN Pb-Bi ALLOYS

INTRODUCTION

Dendrite structures are very frequently observed during the solidification of alloys, and a severe microsegregation pattern exists between the dendrites. This microsegregation pattern has a periodicity of primary and secondary dendrite spacings and it influences the mechanical properties of solidified alloys. During the past thirty years, many theoretical and experimental studies have thus been carried out to characterize primary dendrite spacing as a function of G, V, and C. However, most of these studies are carried out for eutectic phase diagrams. In this section, we shall report our studies on primary dendrite spacing in peritectic alloys of the Pb-Bi system. If primary spacings are determined by conditions ahead of the dendrite tip region, the influence of experimental variables should be the same in peritectic and eutectic systems.

In the Pb-Bi system, studied here, Bi is lighter than Pb so that the vertical density driven convection should be present in this system at low velocities. Earlier studies by Mason et al. [1] in the Pb-Sn system showed that the relationship between primary spacing, λ, and temperature gradient, G, was significantly influenced by the convection effects in that the slope of ln λ vs. ln G decreased as the velocity was decreased. No such change in the slope was observed for Pb-Au and Pb-Pd systems [2]. Consequently, it is desirable to carry out experimental studies in a system in which convection effects are similar to those in the Pb-Sn system.

In Pb-Bi system, α dendrites form for compositions of Bi < 35.0 wt.%. However, for compositions of Bi > 35.0 wt.%, β dendrites form. Our aim is also to study the relative primary spacings of α and β dendrites, and characterize the change in primary spacing that occurs as $\alpha \rightarrow \beta$ transformation occurs.

LITERATURE REVIEW

In directional solidification experiments, both the growth velocity, V, and the temperature gradient in the liquid, G, may be independently controlled. Several directional solidification studies have been carried out to characterize primary dendrite spacing, λ, as a function of G, V and C_∞ [1-10]. Most studies have shown that the primary dendrite spacing decreases as the growth rate or temperature gradient is increased. Various experimental data have thus been correlated with an empirical equation of the form:

$$\lambda = AG^{-a}V^{-b} \tag{1}$$

where a and b are constants and the value of A includes the composition dependence. The first significant theoretical model was proposed by Hunt [11], who carried out a global mass balance that correlated primary dendrite spacing with the dendrite tip radius. His result can be expressed as

$$\Lambda = 4\sqrt{2}\left(\frac{C\tau}{C_\infty} - \frac{GD}{Vk_o\Delta T_o}\right) \tag{2}$$

where Λ is a dimensionless parameter and equal to $\lambda^2 G/Rk_o\Delta T_o$. Hunt [11] then substituted the tip radius value from Equation (2) into a simplified Burden-Hunt [12] equation for dendrite tip undercooling. A minimum undercooling criterion was then used to characterize the primary dendrite spacing as

$$\lambda = B\, G^{-\frac{1}{2}}\, V^{-\frac{1}{4}}\, C^{\frac{1}{4}} \quad . \tag{3}$$

This theoretical relationship could not explain the experimental results over the range of G and V values. In particular, Mason et al. [1] observed that in the Pb-Sn system (1) the exponent of G is not constant, but is a function of velocity; (2) at constant C and G, the relationship $\lambda \alpha V^{-a}$ is valid only at higher velocities. As V is decreased, the spacings tend to become constant and even begin decreasing; (3) at constant C and constant low V, below 10 μm/s, λ also is found to increase with decreasing G, with a smaller value of the exponent than predicted by Equation (3). Klaren et al. [13] and Somboonsuk et al. [14] have carried out detailed experimental studies in the Pb-Sn and in the succinonitritic acetone systems, respectively. They found that λ does not continually increase with decreasing growth rate, but goes through a maximum. Only at high velocities did they find the relation $\lambda \alpha V^{-b}$ for constant G to hold true.

Kurz and Fisher [15] and Trivedi [16] subsequently used a marginal stability criterion to characterize λ. By substituting the stability criterion in Equation (2), Trivedi [16] found the following relationship:

$$\Lambda = 4\sqrt{2}\, \mathcal{A}\, \frac{L}{p^2} \tag{4}$$

where L is a constant which depends on the value of the harmonic of the perturbation and $\mathcal{A}$ is a dimensionless constant equal to $\Upsilon V/2\Delta S\Delta k\Delta T_o$. Equation (4) predicts that λ goes through a maximum as a function of

the growth rate. Such a maximum has been observed experimentally by a number of investigators [1, 2, 13, 14]. The maximum in λ has been correlated with the onset of the dendrite-to-cell transition [14].

Equation (4) also predicts that λ is proportional to $G^{-\frac{1}{2}}$. Experimental studies by McCartney and Hunt [10], Mason et al. [1] and Somboonsuk et al. [14] have confirmed the validity of this prediction. Mason et al. [1] found deviation from $G^{-\frac{1}{2}}$ for lead dendrite growth in the Pb-Sn system. However, this deviation appears to be due to the presence of convection in this system.

The effect of composition on primary dendrite spacing was found to be quite small by Klaren et al. [13] for a temperature gradient of 350 K/cm. Mason et al. [1] results also confirm this observation. Spittle and Lloyd [17] studied primary dendrite spacing in various lead-tin alloys with compositions in the range of 20-40 wt.% tin. At $V = 0.12$ μm/s and $G = 66$ K/cm, they found that the dendrite spacing decreases with increasing composition. This result may be due to the large convection effects which will be present under such a small velocity condition.

EXPERIMENTAL RESULTS

The experimental apparatus and procedure used in this study are identical to those described in Section I. Directional solidification studies were carried out for alloy samples of 10.5 cm length and 5 to 7 cm of sample was solidified before quenching. Primary spacings were measured from the transverse section by using the method described by Jacobi and Schwerdtfeger [3]. For dendrite spacing measurements, the transverse section was taken at about one inch behind the advancing tip. However, for cell spacings, the transverse section close to the cell tip was taken since cells tend to coarsen with time.

The results obtained in this study are summarized in Table 1. The alloy compositions studied were 24, 26, 28, 30, 33 and 35 wt.% Bi within the peritectic region, and 40 and 50 wt.% Bi within the hypoeutectic region. In this experiment, we did not consider the hypereutectic alloys because the primary bismuth phase in these alloys exhibits a faceted structure. The temperature gradients were varied from 3.8 to 35 k/mm, and the growth rates were varied from 0.75 to 500 μm/s.

Growth Rate Dependence

The general variation in primary spacing (λ) with growth rate is illustrated in Figure 1 for α-dendrite growth in the Pb-30 wt.% Bi alloys which were directionally solidified at G = 21.6 K/mm. The variation in primary spacing in the ln λ versus ln V plot is essentially linear for high growth rates, but it flattens out at lower velocities

Table 1. Summary of Pb-Bi experimental data

C (wt.% Bi)	G (k/mm)	V (μm/s)	λ (μm)
24	10.4 ± 1.0	5	278
		7.5	283
		10	275
24	10.4 ± 1.0	25	236
		50	189
		100	133
		200	103
		7.5	169
		10	178
24	27.2 ± 1.0	25	159
		50	144
		100	95
		200	72
		5	256
		7.5	267
		10	263
26	10.6 ± 1.0	25	227
		50	191
		100	135
		200	103
		5	192
		10	211
		25	156
26	27.8 ± 1.0	50	145
		100	88
		200	72
		5	287
		7.5	281
		10	286
		25	230
28	11.0 ± 1.0	50	189
		100	135
		200	107

Table 1. Continued

C (wt.% Bi)	G (k/mm)	V (μm/s)	λ (μm)
28	28.0 ± 1.0	5	201
		7.5	198
		10	201
		15	185
		25	172
		50	137
		100	99
		200	73
30	3.8 ± 0.5	5	437
		7.5	393
		10	385
		25	366
		50	309
		100	210
		200	159
30	11.4 + 1.0	5	268
		7.5	268
		10	270
		25	236
		50	182
		100	129
		200	95
		700	52
30	21.5 ± 1.0	0.5	planar
		0.75	89
		1	142
		1.5	245
		2.5	258
		5	236
		7.5	230
		10	246
		25	188
		50	154
		100	107
		200	78
		500	51

Table 1. Continued

C (wt.% Bi)	G (k/mm)	V (μm/s)	λ (μm)
30	28.0 ± 1.0	5	192
		7.5	213
		10	198
		25	186
		50	129
		100	102
		200	71
		500	46
30	32.0 ± 1.0	1	68
		3	139
		5	158
		10	179
		25	165
		50	118
		100	81
		200	59
33	12.0 ± 1.0	5	278
		7.5	285
		10	275
		25	232
		50	188
		100	133
		200	101
33	29.0 ± 1.0	5	179
		10	204
		50	133
		100	95
		200	69
40	13.0 ± 1.0	1	133
		2.5	329
		5	289
		10	252
		25	213
		50	140
		100	119
		200	82

Table 1. Continued

C (wt.% Bi)	G (k/mm)	V (μm/s)	λ (μm)
45	13.5 ± 1.0	1	137
		5	283
		10	257
		25	215
		50	152
		100	115
		200	78
50	12.5 ± 1.0	0.5	102
		3	259
		5	270
		10	215
		25	188
		50	127
		100	96
		200	70
		400	38

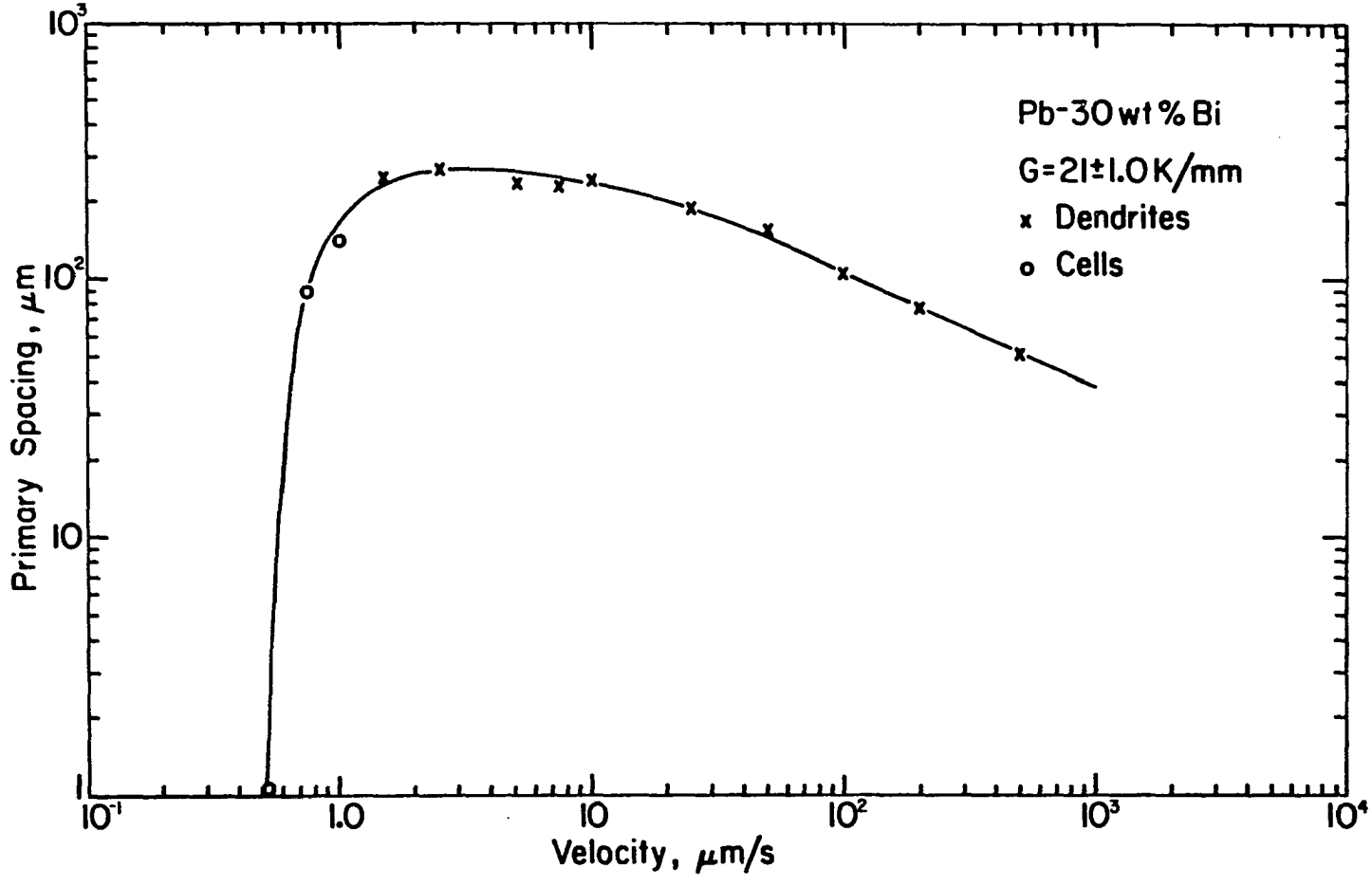

Figure 1. The variation in primary spacing (λ) of α dendrites with growth rate in Pb-30 wt.% Bi alloys at G = 21 K/mm

and then goes down as the velocity is further reduced. A sharp decrease in λ is observed at low velocities until the transition from α dendrite to planar β phase occurs as described in Section I. A similar growth rate dependence of primary spacing is observed for β-phase dendrites, as shown in Figure 2. The high velocities, $\lambda \alpha V^{-b}$, and the values of b for Pb-30 wt.% Bi are listed in Table 2 for different temperature gradient conditions.

Table 2. Least squares fit of λ versus V data for $\lambda \alpha V^{-b}$; velocity between 50 and 700 μm/s

G (K/mm)	b	Standard deviation in the exponent b
3.8	0.48	0.039
11.4	0.47	0.008
21.6	0.48	0.018
27.7	0.46	0.041
32.1	0.50	0.026

The changes in microstructure which occur as the velocity is increased are shown in Figure 3 for the experimental conditions of Figure 1. Figures 3a and 3b show that, at low velocities, a cellular structure is obtained. For this case, the primary spacing is seen to increase with the increase in velocity. Figures 3c-3f show dendritic structures and the primary spacing is found to decrease as the velocity is increased. The maximum in primary spacing, thus, correlates with

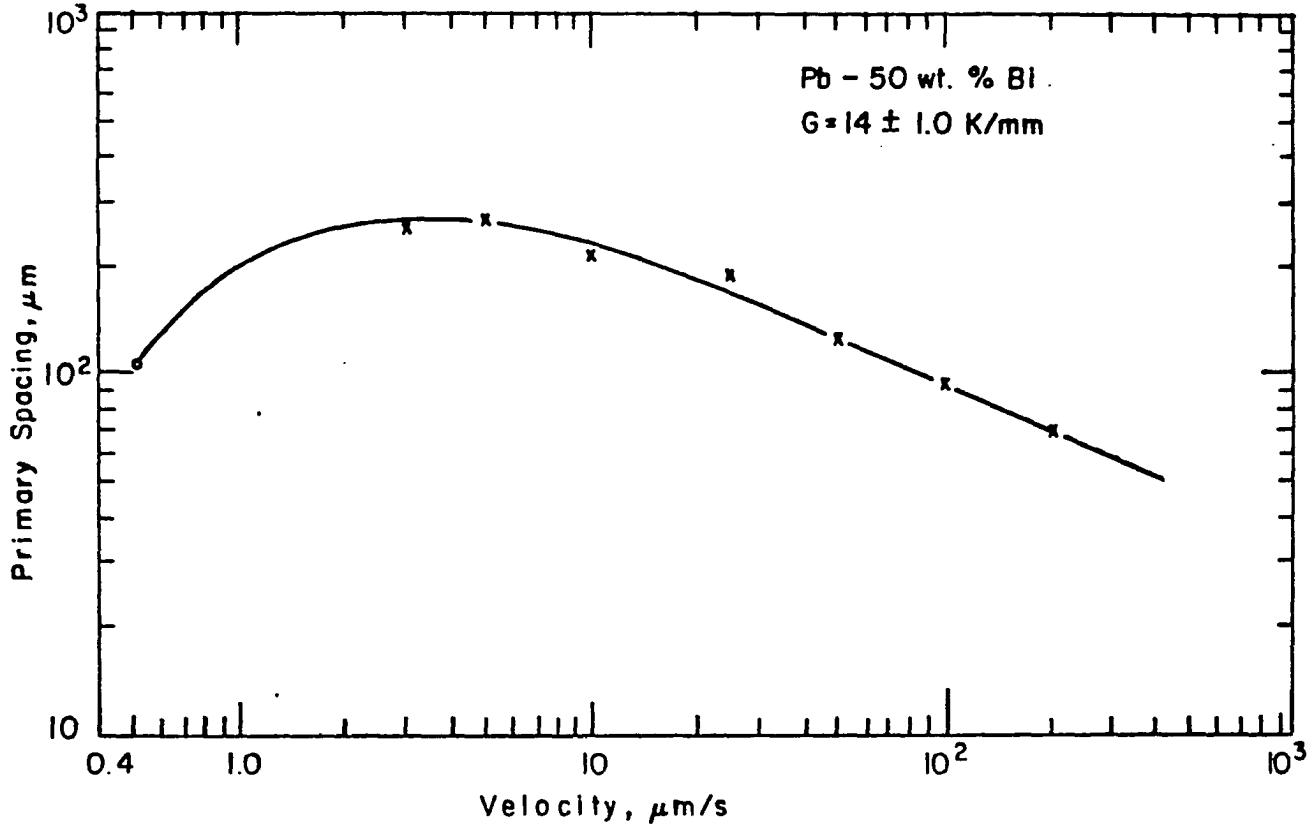

Figure 2. The variation in primary spacing of β dendrites with growth rate in Pb-50 wt.% Bi alloys at G = 14 K/mm. x = dendrite; o = cell

Figure 3. The transverse microstructure for Pb-30 wt.% alloys at G = 21.5 K/mm for velocities (μm/s) of: (a) 0.75, (b) 1, (c) 10, (d) 25, (e) 50 and (f) 100. M = 28.54 X; sample diameter 6 mm ((c) - (f))

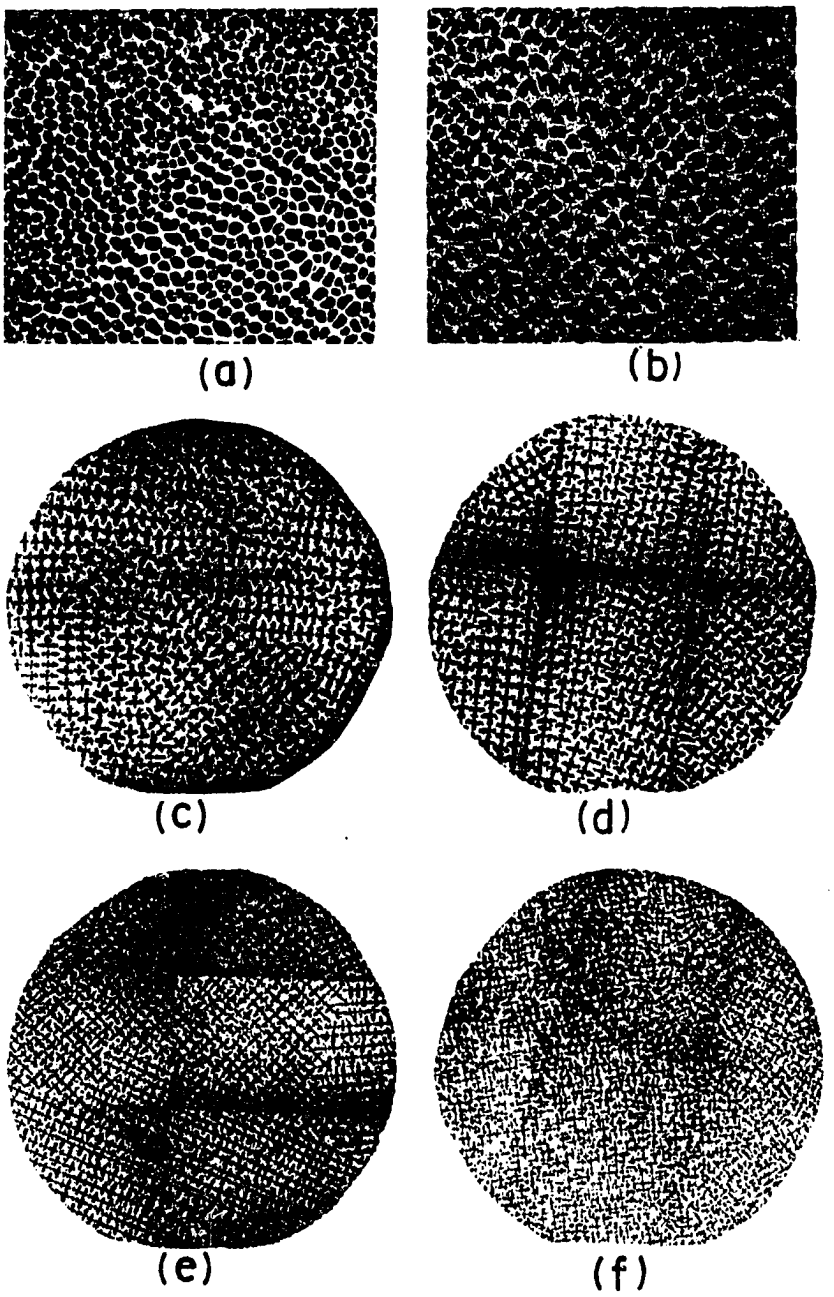
(a)
(b)
(c)
(d)
(e)
(f)

the dendrite-to-cell transition as reported earlier by Somboonsuk et al. [14].

Temperature Gradient Effect

The dendritic spacings were studied over a range of temperature gradients at a series of constant velocities. The primary dendrite spacing is found to increase as the temperature gradient is lowered, as shown in Figure 4. This effect of temperature gradient on primary spacing of α-dendrites is shown in Figure 5 for Pb-30 wt.% Bi alloy. The data form a family of straight lines with a relationship of the form $\lambda \alpha G^{-a}$. The exponent, a, of this family of lines is nearly constant for velocities above 50 μm/s. However, at lower velocities, the exponent a is found to decrease significantly. This decrease in the exponent value is similar to the one found earlier by Mason et al. in the Pb-Sn system. Since Sn and Bi are both lighter than lead, the decrease in the value of the exponent a at lower growth rates appears to be due to the density driven convection effects which will be present in these systems at low velocities. The values of the exponent a, for Pb-30 wt.% Bi alloys, are given in Table 3 for different velocity conditions.

The changes in microstructure which occur as the temperature gradient is increased are shown in Figure 6. For the temperature gradient values studied in this investigation, the microstructures show that the solid-liquid interface is dendritic in nature.

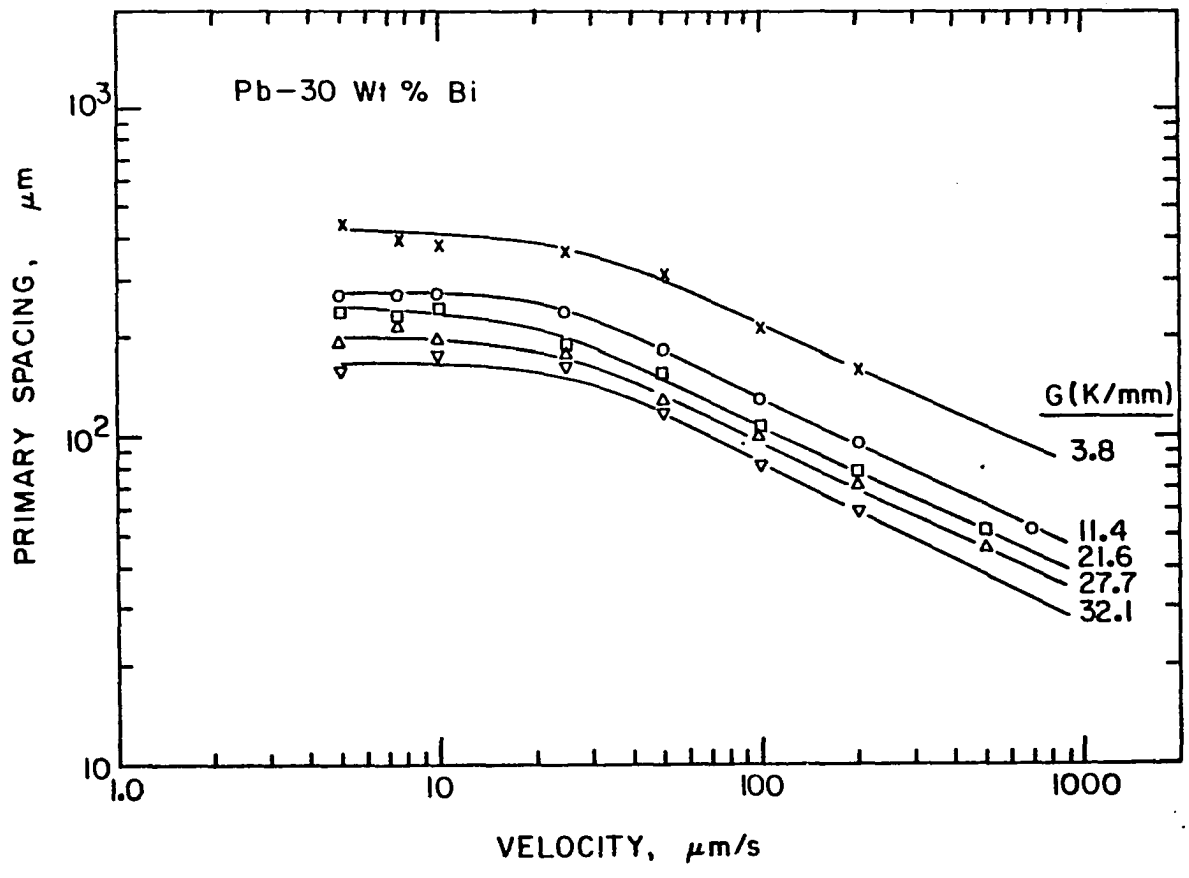

Figure 4. Primary spacing versus growth rate for Pb-30 wt.% Bi alloys at at series constant temperature gradients

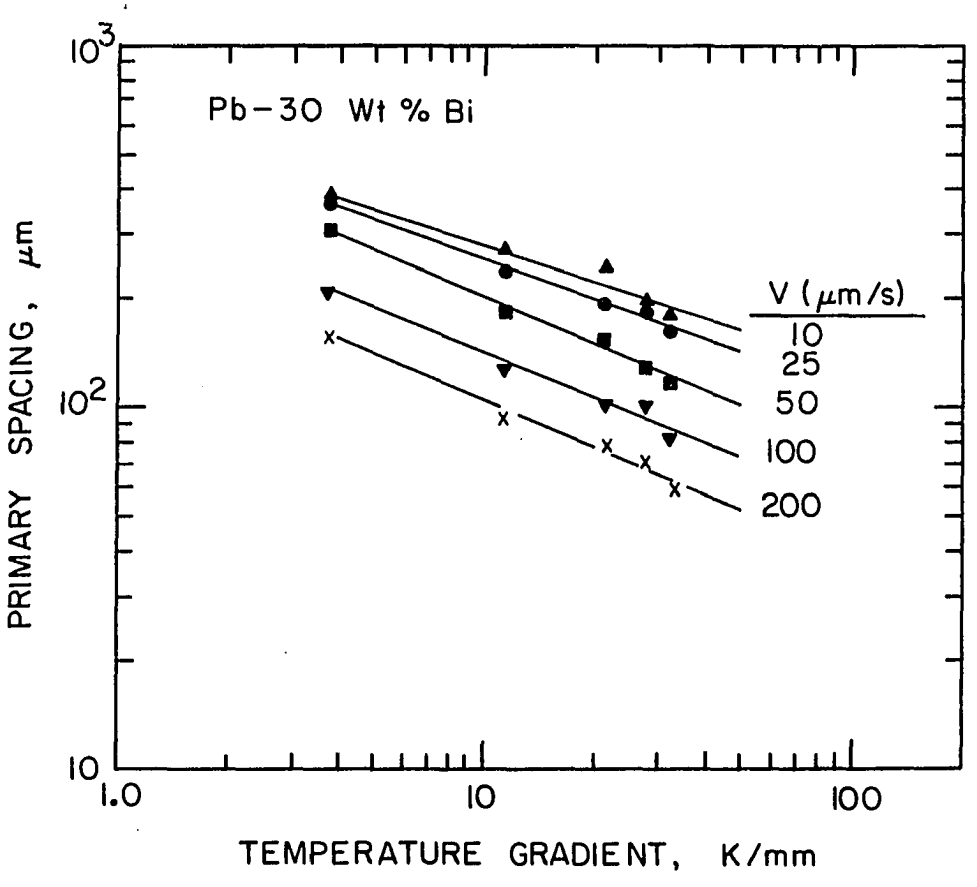

Figure 5. Primary spacing versus temperature gradient for Pb-30 wt.% Bi alloys at a series of constant growth rate values

Figure 6. The transverse microstructures for Pb-30 wt.% Bi with V = 50 μm/s at G (K/mm) of: (a) 3.8, (b) 11.4, (c) 21, and (d) 27.7. Sample diameter 6 mm

(c)
(p)
(d)
(q)

Table 3. Least squares fit of λ versus V data for Pb-30 wt.% Bi alloys to the relationship $\lambda \alpha G^{-a}$

V (μm/s)	a	Standard deviation in the exponent a
10	0.33	0.080
25	0.36	0.043
50	0.43	0.051
100	0.42	0.076
200	0.43	0.060

The changes in microstructure which occur as the temperature gradient is increased are shown in Figure 6. For the temperature gradient values studied in this investigation, the microstructures show that the solid-liquid interface is dendritic in nature.

Alloy Composition Effect

Experiments were run with 24, 26, 28, 30, 33 and 35 wt.% Bi-Pb alloys in the peritectic region, and 40, 45 and 50 wt.% Bi-Pb alloys in the hypoeutectic region. These results are shown in Figures 7 and 8 for α and β dendrites, respectively. For constant G and V, the effect of composition on primary α-dendrite spacing in the peritectic region was found to be quite small as shown in Figures 9 and 10. For the same gradient and velocity values, the primary β-dendrite spacing is found to be smaller than that of α dendrite. Furthermore, β-dendrite spacing appears to decrease with increasing alloy composition. The changes in microstructure with composition are shown in Figure 11.

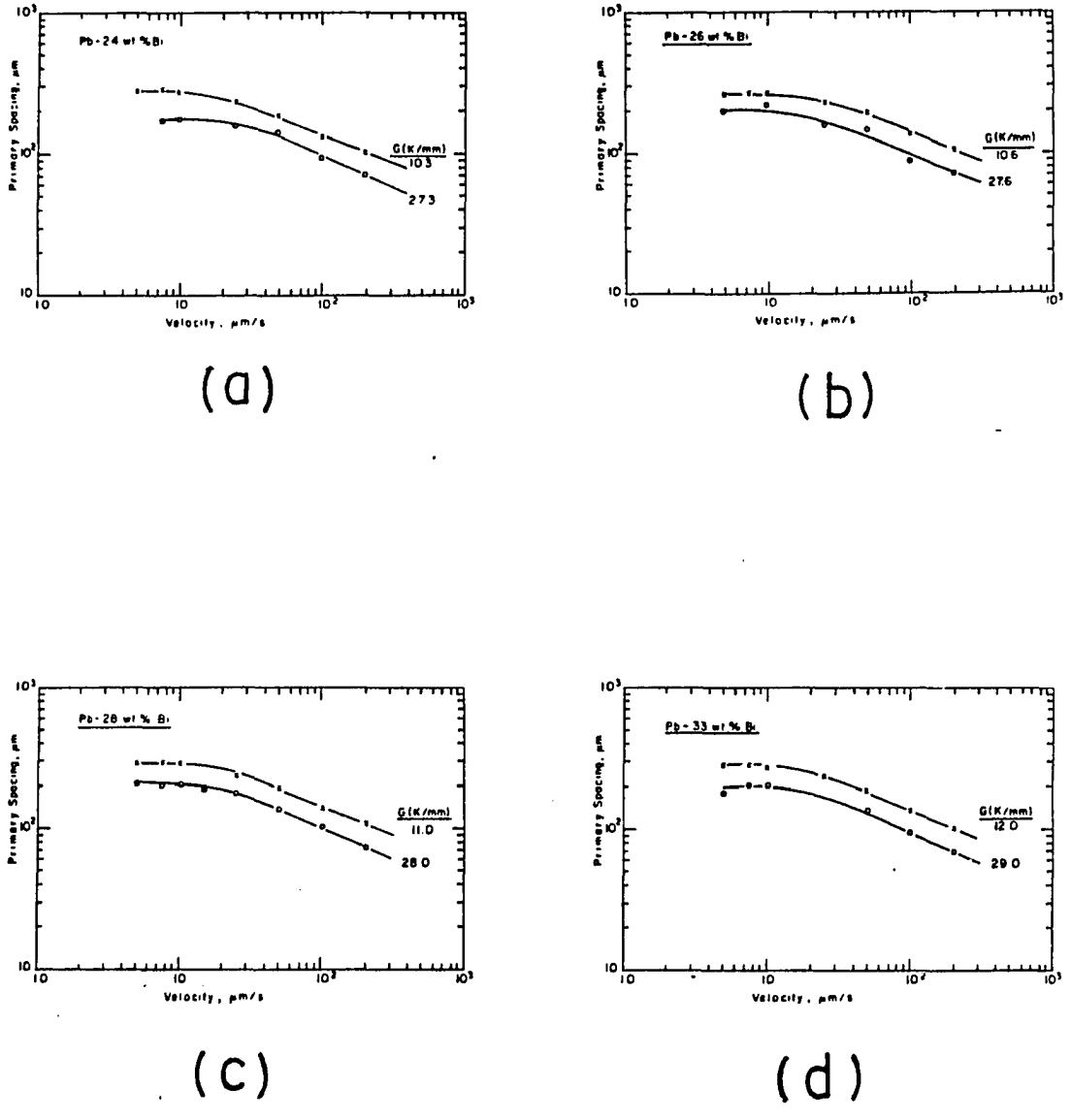

Figure 7. The variation in primary spacing with growth rate at G = 11.0 and 28.0 K/mm conditions for alloy compositions (wt.% Bi): (a) 24, (b) 26, (c) 28, and (d) 33

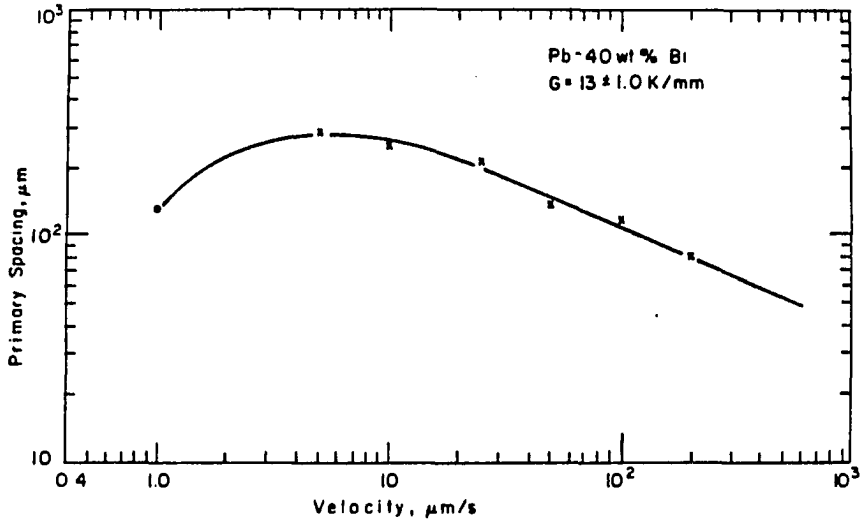

(a)

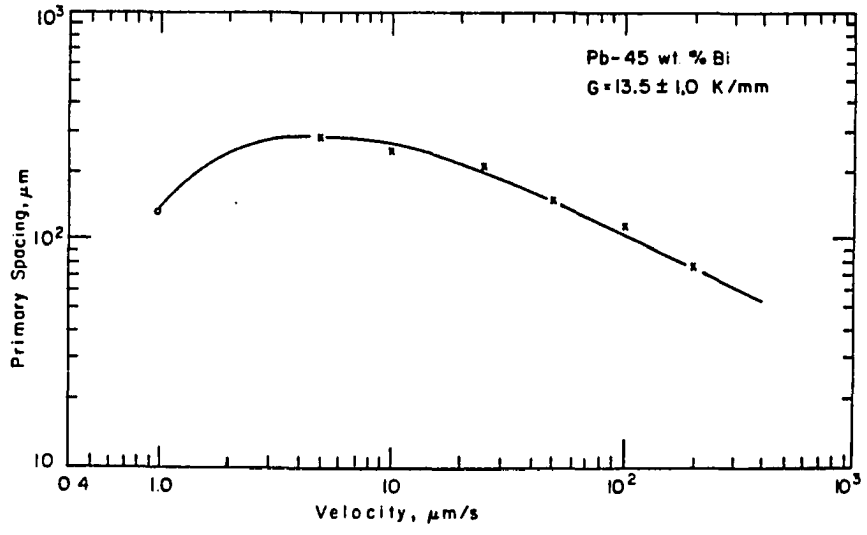

(b)

Figure 8. The variation in primary spacing with growth rate for alloy compositions (wt.% Bi): (a) 40, (b) 45, at G = 13 K/mm condition

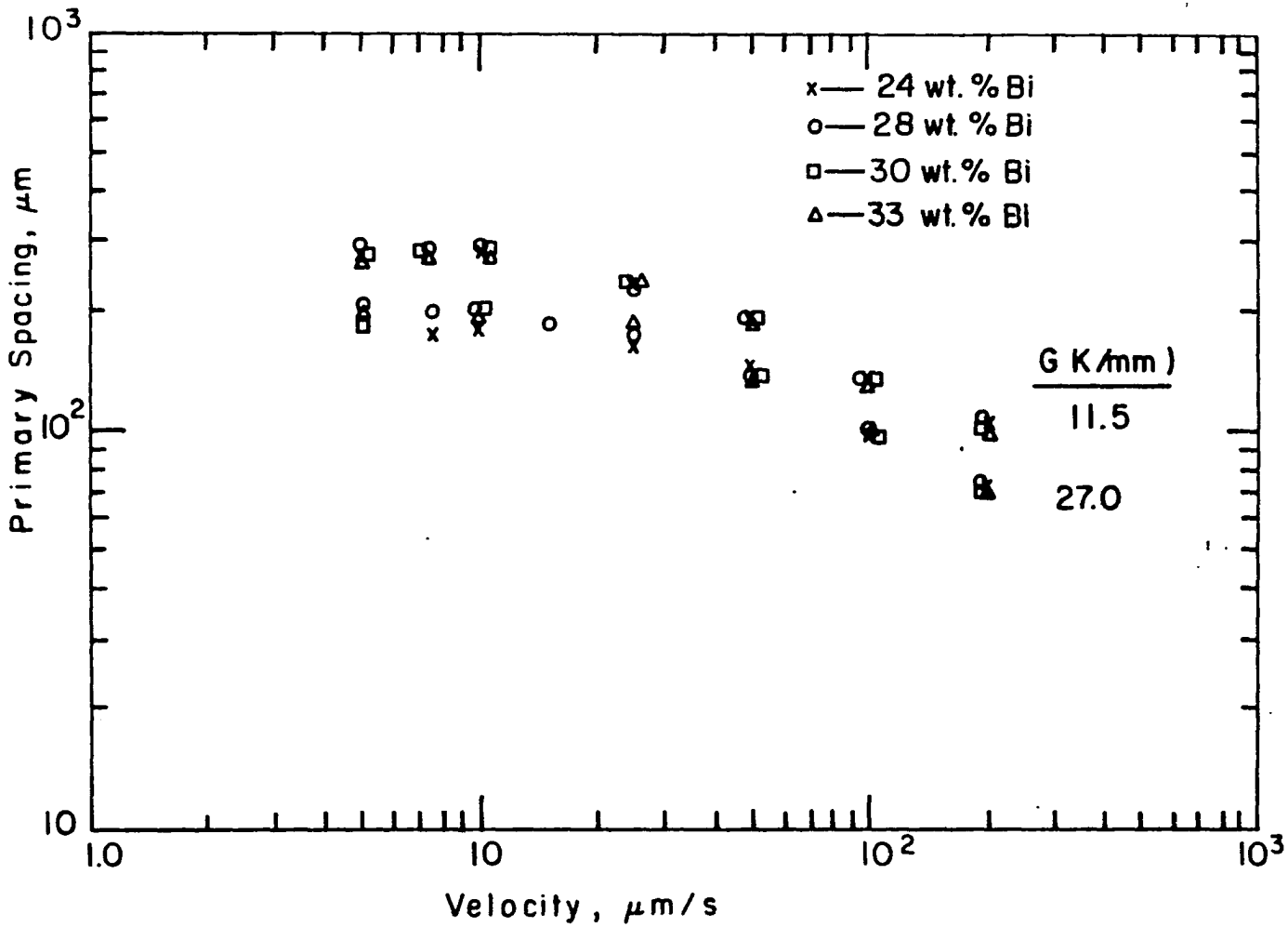

Figure 9. λ versus V data for several compositions of Pb-Bi alloys at G = 11.5 and 27.0 K/mm conditions

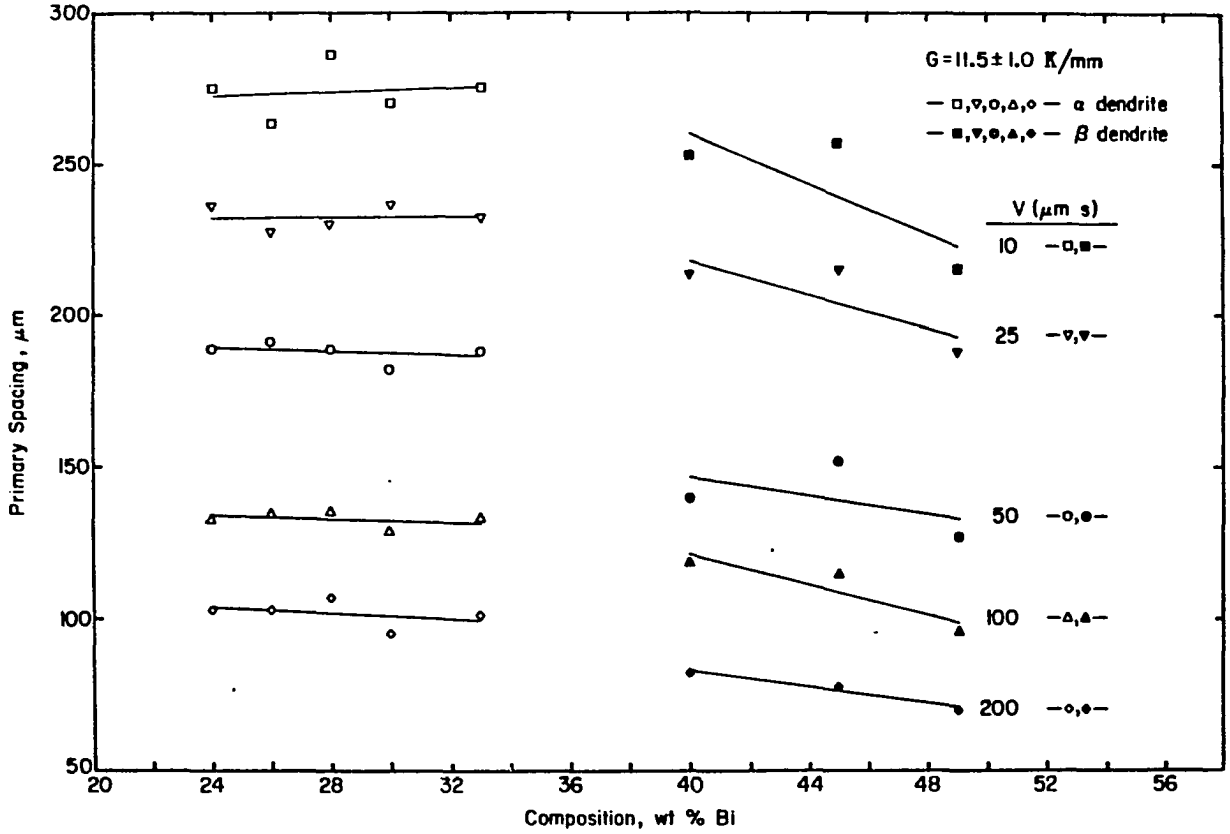

Figure 10. The variation in primary spacing with alloy composition of G = 11.5 K/mm and a series of constant V values

Figure 11. The transverse microstructure for alloy compositions (wt.% Bi): (a) 24, (b) 26, (c) 28, and (d) 30, at G = 11.4 K/mm and V = 25 μm/s conditions. Sample diameter 6 mm

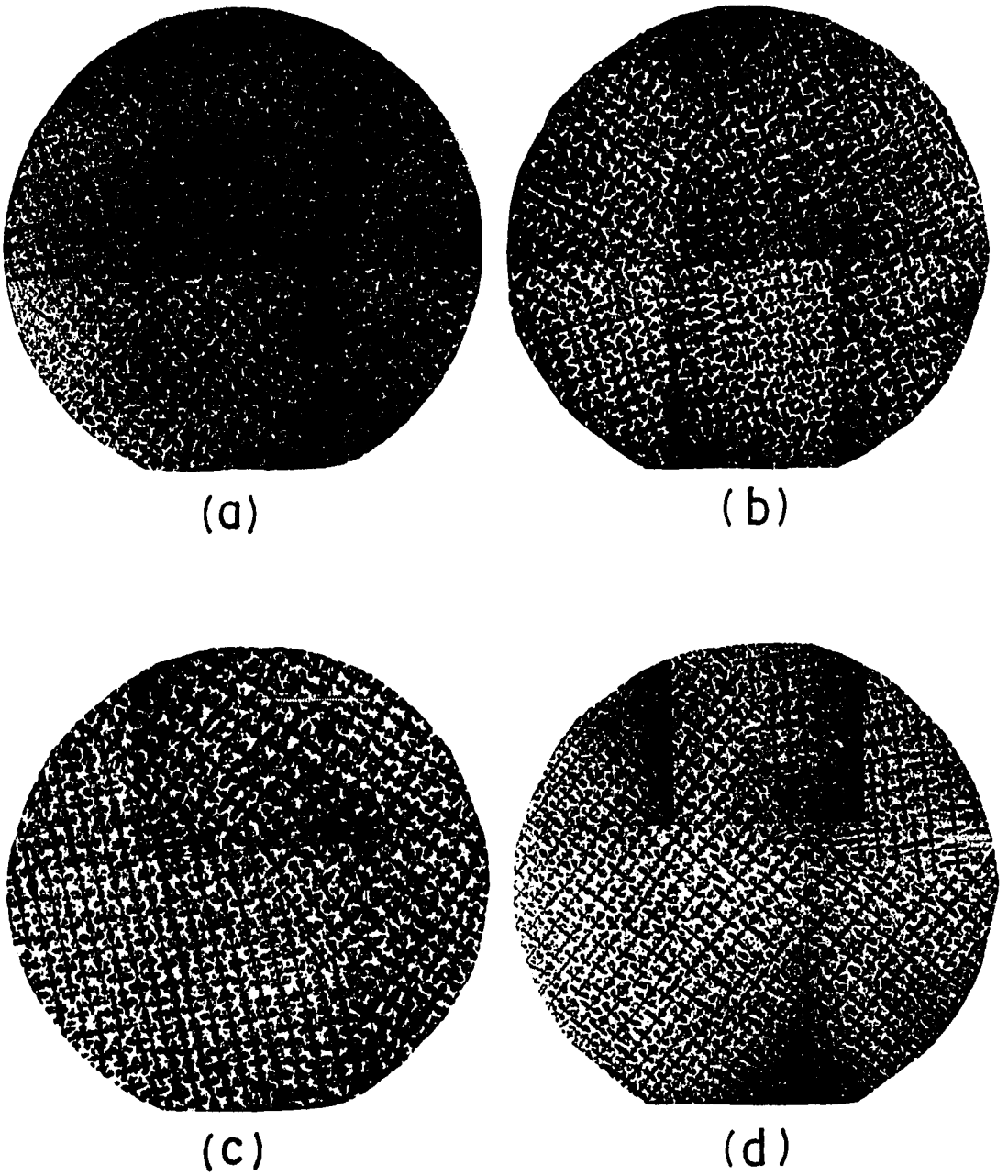
(a)
(b)
(c)
(d)

DISCUSSION

Experimental results were obtained in these studies for C_∞ < 33.0 wt.%, and these results were found to be quite similar to those obtained by Mason et al. [1] in the Pb-Sn system. In the present case, the interdendritic region for α-dendrites consisted of β-phase, as shown in Figure 12. Consequently, the effect of the nature of interdendritic phase does not appear to influence the primary dendrite spacing. Thus, primary spacings are controlled by the conditions in the liquid region near and ahead of the dendrite tip region.

The effect of interdendritic phase was found to be quite significant for the alloys in the hyper-peritectic region. Consequently, it was difficult to measure primary spacing in hyper-peritectic alloys.

The primary spacings of β dendrites were found to be significantly smaller than the primary spacings of α dendrites under identical conditions of G and V, as seen in Figure 10. This can be rationalized by examining Equation (4), which shows that

$$[(\lambda_1)_\alpha/(\lambda_1)_\beta]^2 \, \alpha[(\rho)_\beta/(\rho)_\alpha] \sim [(k_o\Delta T_o)_\alpha/(k_o\Delta T_o)_\beta]^{\frac{1}{2}} . \qquad (4)$$

Since the value of the ratio on the right-hand side is larger than unity, $(\lambda_1)_\alpha > (\lambda_1)_\beta$. The effect of composition on the primary spacing of α dendrites is quite small. However, the primary spacing of β-phase is found to decrease with the increase in composition. The decrease in spacing is more pronounced at low velocity values. Since convection effects increase with composition, high Bi concentration

Figure 12. Longitudinal and transverse sections of Pb-30 wt.% Bi alloy at G = 11.5 K/mm and V = 6 μm/s conditions:

(a) longitudinal sections, M = 28.54x;
(b) transverse section at position n-n in (a) shows the peritectic reaction around the α-dendrite, M = 78.6x;
(c) transverse section at position m-m in (a) shows no peritectic reaction, M = 78.6x

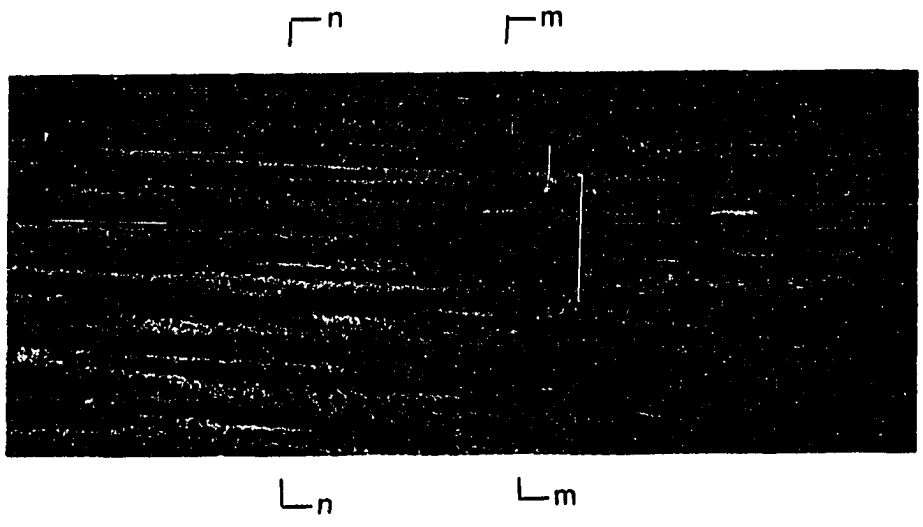

a

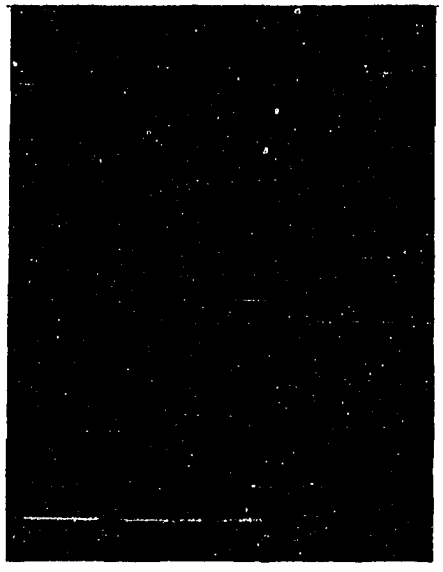

b

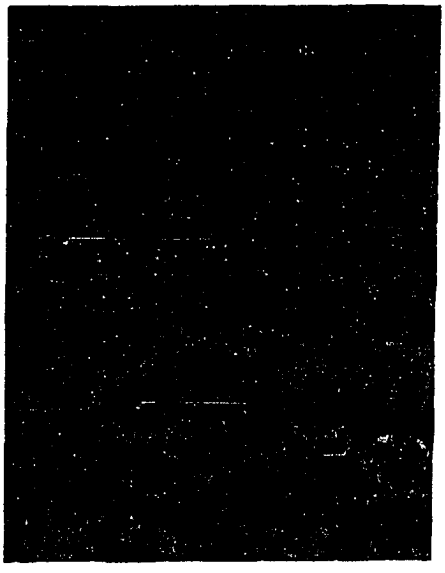

c

alloys should have large convection effects. Thus, the decrease in λ appears to be due to convection effects in the liquid. The microstructure of β-dendrite shows an interesting feature. In general, the phase of hcp structure will exhibit a six-fold branched microstructure. However, in all experiments, the β-dendrites in the Pb-Bi system exhibited five-fold branches, as shown in Figure 13. The six-fold branches of β-dendrites were not observed, even in the transverse section taken near the tip. Coarsening phenomena may cause a six-fold symmetry to degenerate to the five-fold symmetry observed experimentally. However, such a coarsening phenomenon, if it exists, must be very rapid near the tip region.

Figure 13. The microstructure of β dendrites magnification in (a) 42x, (b) 345x

(a)

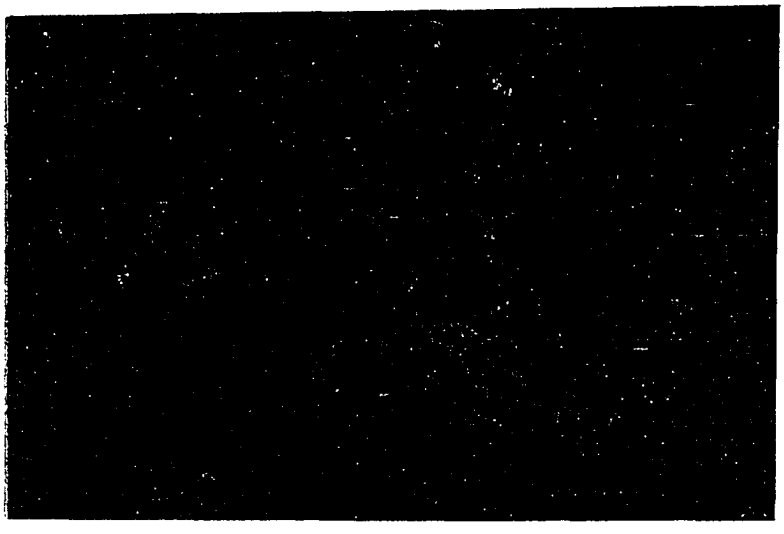

(b)

CONCLUSIONS

1. It has been shown that the characteristics of primary spacing for the peritectic alloys are identical to those for the eutectic alloys.

2. Only at high velocities do we find the relationship $\lambda \alpha G^{-a}$ for constant composition and velocity to hold true. The value of the exponent is found to depend on velocity.

3. Only at higher velocities do we find the relationship $\lambda \alpha V^{-b}$ for constant composition and temperature gradient to hold true. The value of exponent b is about 0.45 ~ 0.50. It is also found that the primary spacing at constant G and composition become nearly independent of velocity for velocities around 10 μm/s.

4. For constant G and V, the effect of composition on primary spacing in peritectic region was found to be quite small. For the same gradient and velocity values, the primary β-dendrite spacing is found to decrease with increasing alloy composition.

REFERENCES

1. Mason, J. T., Verhoeven, J. D. and Trivedi, R. J. Cryst. Growth 1982, 59, 516.

2. Mason, J. T., Verhoeven, J. D. and Trivedi, R. Met. Trans. A (in press).

3. Jacobi, H. and Schwerdtfeger, K. Met. Trans. A. 1976, 7A, 811.

4. Dann, P. C., Eady, J. A. and Hogan, L. M. J. Australian Inst. Metals 1974, 19, 140.

5. Young, K. P. and Kirkwood, D. H. Met. Trans. A 1975, 6, 197.

6. Taha, M. A. Met. Sci. 1979, 13, 9.

7. Bell, J. A. E. and Winegard, W. C. J. Inst. Met. 1963, 92, 357.

8. Okamoto, T. and Kishitake, K. J. Cryst. Growth 1975, 29, 131.

9. Sharp, R. M. and Hellawell, A. J. Cryst. Growth 1971, 11, 77.

10. McCartney, D. G. and Hunt, J. D. Acta Met. 1981, 29, 1851.

11. Hunt, J. D. Solidification and Casting of Metals. The Metals Society, London, 1979, p. 3.

12. Burden, M. H. and Hunt, J. D. J. Cryst. Growth 1974, 22, 109.

13. Klaren, C. M., Verhoeven, J. D. and Trivedi, R. Met. Trans. A. 1980, 11, 1853.

14. Somboonsuk, K., Mason, J. T. and Trivedi, R. Met. Trans. A. 1984, 15, 967.

15. Kurz, W. and Fisher, D. J. Acta Met. 1981, 29, 11.

16. Trivedi, R. Met. Trans. A 1984, 15, 977.

17. Spittle, J. A. and Lloyd, D. M. Solidification and Casting of Metals. The Metals Society, London, 1979, p. 15.

SECTION III. FORMATION OF BAND STRUCTURES IN Pb-Bi PERITECTIC ALLOYS

INTRODUCTION

Band structures have been found in a number of peritectic systems under controlled solidification conditions [1-5]. However, the precise conditions under which these bands form, and the mechanism for the formation of bands are not clearly understood. For example, Barker and Hellawell [2] observed bands in only two out of the six experiments. Also, Brody and David [3] did not observe band formation in the same system. The purpose of these experiments is to carry out a systematic study of the band structure formation in the lead-bismuth peritectic system and to understand the mechanism of band formation in peritectic systems.

LITERATURE REVIEW

Several investigators [1-6] have reported the observation of band structures in directionally solidificated peritectic alloys. Boettinger [1] found the band structure of Sn-Cd two-phase peritectic alloy under directional solidification conditions. In his paper, the minimum value of G/V as a function of composition required for the solidification of two-phase peritectic alloys with a planar liquid-solid interface was estimated by using simple constitutional supercooling stability criterion. At the value of G/V above this minimum value, the alloys solidified with a planar interface which alternates deposits of α and β phases, transverse to the growth direction. This result is shown in Figure 1. Boettinger explained that the α phase first solidifies until the composition of the liquid at the interface exceeds 3.8 wt.% Cd (Figure 1a). Next, β solidifies until the composition in the liquid at the interface is depleted to less than 3.8 wt.% Cd. Then the α phase solidifies again and the process is repeated. Barker and Hellawell [2] found two of the six specimens were frequently banded in the Pb-Bi peritectic alloys at slow growth rates ($V \cong 0.025$ μm/s) and steep temperature gradients. They rationalized that the band formation occurs because of the inevitable vibrations at such slow growth rate. Brody and David [3] also found the band structures in the Sn-Cd system, the same as Boettinger's results, but they did not find the band structure in the Pb-Bi system. Titchener and Spittle [5] found the band structures in a Sn-15 wt.% Sb alloy unidirectionally solidified at a rate of 7.1 x

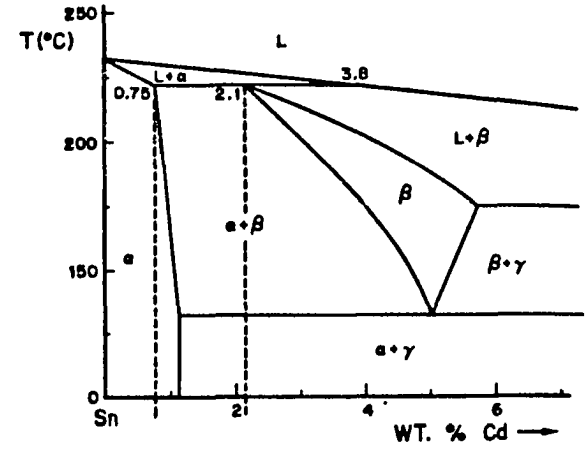

(a)

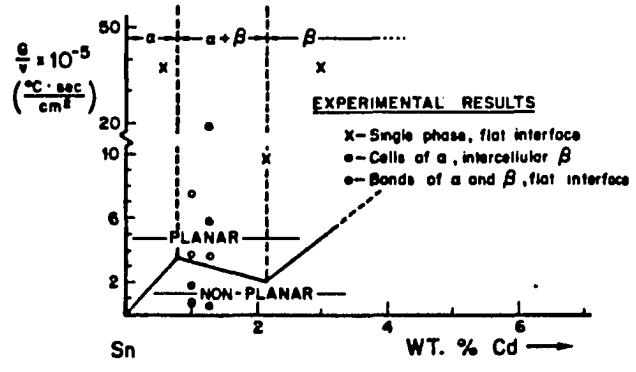

(b)

Figure 1. A correlation between the phase diagram and solidification structures.

a) Phase diagram of the Sn-Cd peritectic system.
b) Critical G/V ratio vs. Cd concentration for planar liquid-solid interface, as predicted by the constitutional supercooling criterion

10^{-6} cm/s with a gradient of 550°C/cm, and in a Zn-3.5 wt.% Cu alloy unidirectionally solidified at 2.9 x 10^{-5} cm/s with a gradient of 250°C/cm. Titchener and Spittle discussed these band structures separately. In the Sn-Sb system, they considered an alloy of composition C_x (Figure 2) which will solidify with a planar interface. The first solid to freeze out would be β' and as freezing progressed, the liquid adjacent to the solid-liquid interface became continuously richer in the solvent tin. Ultimately, the tin concentration reached a value equal to or more probably greater than 91 wt.% Sn (i.e. C_2) whereupon the (Sn) phase could be nucleated on the β' surface. If it did, and as a consequence, the β' surface was covered by (Sn), subsequent direct freezing of (Sn) from the melt would cause the liquid boundary layer concentration profile to change. As the (Sn) phase solidified, the boundary layer became richer in the solute antimony until nucleation and growth of β' occurred. Continuous alternate deposition of β' and (Sn) would therefore be formed to give a band structure. In Zn-Cu alloys, at the growth rate of 2.9 x 10^{-5} cm/s, the ε-dendrite morphology changed from a branched to rod type. Growth of the ε dendrites would continue until the zinc concentration ahead of the tips reached a value equal to or greater than C_2. The liquid and ε phase then reacted peritectically leading to the termination of ε growth. Growth of η then continued until the boundary layer was sufficiently depleted in zinc for the ε to be nucleated again on the η surface. The cyclic formation of bands of ε + η and η presumably continued until such time that the bulk liquid composition approaches C_2 when the remaining liquid

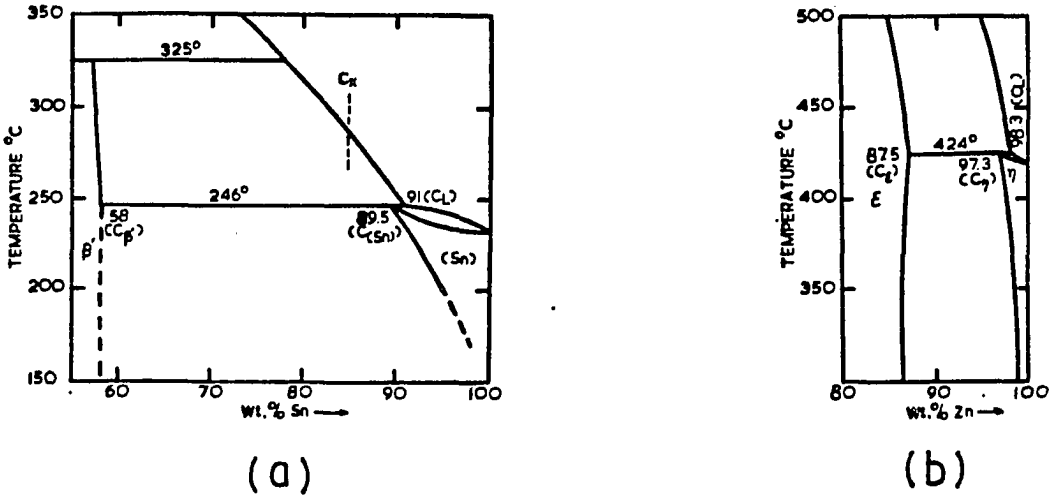

Figure 2. Portions of the binary phase diagrams of a) Sn-Sb and b) Zn-Cu systems

solidified as η phase. Ostrowski and Langer [4] observed a banded structure of alternate layers of $\eta + \varepsilon$ and η lying perpendicular to the growth direction on an Ag-Zn alloy with 10 wt.% Ag at a value of $G/V = 8 \times 10^6$ [$^oCS/cm^2$]. This band structure formation was explained on the basis of the differences in the thermal coefficients of expansions between the alloy and the quartz tube. They explained that the large difference in the coefficients of thermal expansion between the quartz tube and the alloy gave rise to the presence of a small space between the quartz and metal surface. If the same conditions were maintained during the entire solidification process, it would not be possible to observe any effect. However, a steep decline in temperature would occur if contact was suddenly established between the tube and the alloy. This results in an increased degree of constitutional undercooling which would be sufficient for nucleation of the primary phase (ε). This phase was now able to grow and a decrease in undercooling in front of the primary phase stopped its growth because the contact between the alloy surface and the quartz tube ceased shortly afterward as a result of thermal contraction on cooling. Therefore, the temperature gradient in the melt began to increase again, resulting in a one-phase structure. This repeating process gave rise to band structures. Hillert [6] gave an explanation for the banded structure formation with reference to the phase diagram. Figure 3 shows a typical peritectic diagram and it is evident that an alloy of the indicated composition can solidify as pure α at a temperature T_1. If the temperature gradient is successively increased, the temperature of

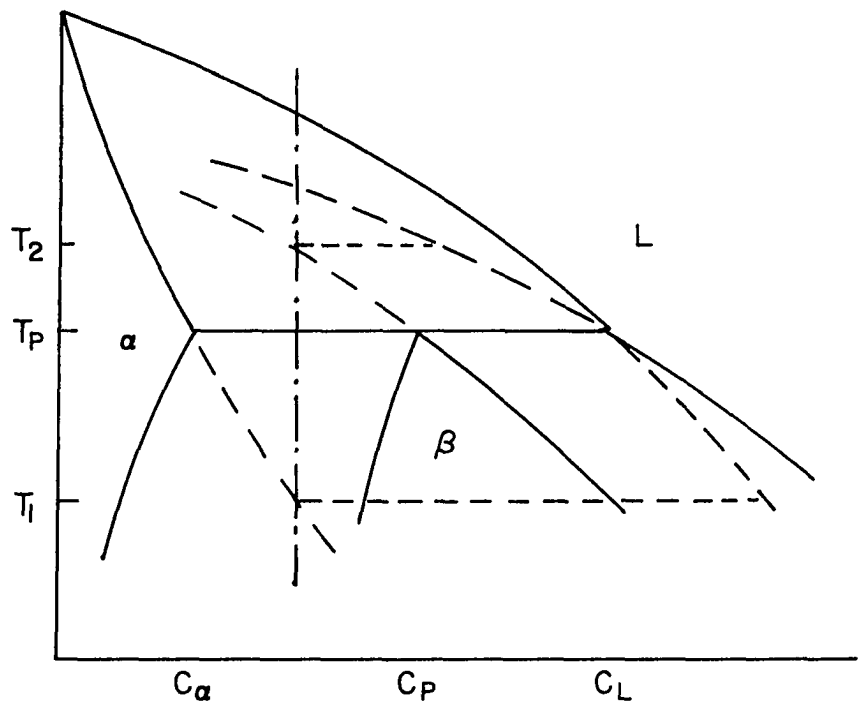

Figure 3. Hypothetical peritectic phase diagram

the solidification front will thus decrease continuously and the dendritic morphology will change to cellular and finally, it will become planar at T_1. However, the extrapolated phase boundaries for the $\beta + L$ equilibrium indicate that, in the absence of α, it should be possible to make the same alloy solidify to pure β with a planar solidification front at T_2 which is higher than T_1. If the β-phase is nucleated, it may thus form a complete layer ahead of the planar α-front. Furthermore, the β-phase in contact with the liquid is not stable with respect to α at the temperature T_2 because it is above the peritectic temperature. As a consequence, if α is nucleated, it may grow along the β/L interface and again form a planar α-front.

EXPERIMENTAL TECHNIQUES

Material preparation and experimental apparatus are identical, as described in Section I. The sample length used in this work is 12.8 cm long. The distances over which the alloy was directionally solidified were varied depending on the specimen composition. The lower bismuth content needed a longer growth length to get the band structure. In this experiment, the specimen compositions were prepared with the concentration of 24, 26, 28, 30, 33 and 35 wt.% Bi, which encompassed the entire range of the peritectic composition in the Pb-Bi system (Figure 4). The temperature gradient used in this section was 21.5 K/mm. The growth rates in this study are 0.4 μm/s, at which the α-phase will grow as a planar interface, as well as 0.5, 0.55, 0.6 μm/s which are slightly higher than the V_{cr} value for the Pb-30 wt.% Bi alloy at G = 21.5 K/mm.

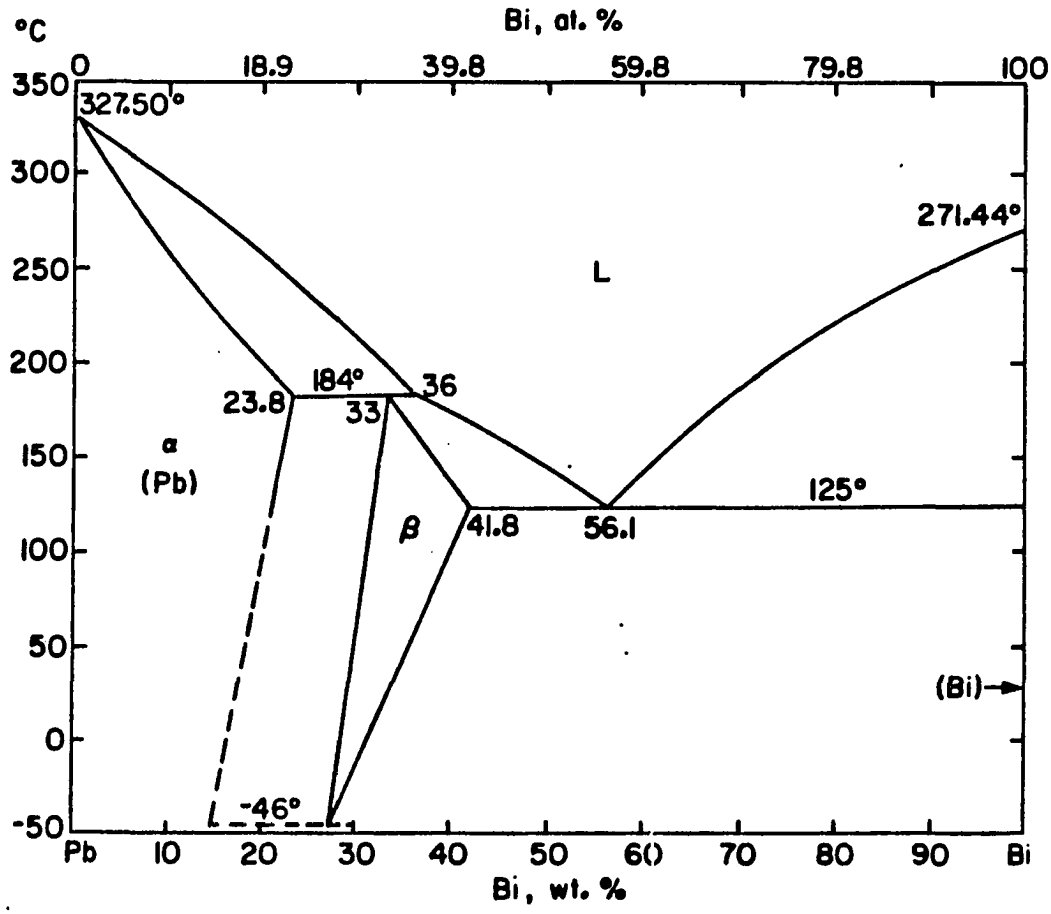

Figure 4. Pb-Bi phase diagram

EXPERIMENT RESULTS

The band structures have been found in Pb-Bi alloys of peritectic composition which are solidified under controlled unidirectional solidification conditions. The specimens were run under the conditions that the α-phase will grow as a planar front. As the specimens solidified over a sufficient length, the band structures were observed between the single α phase and single β phase. The microstructures of the band structure for a series of alloy compositions are shown in Figure 5. It is seen that the number of bands formed increased as the alloy composition was increased. An entire microstructure of a Pb-35 wt.% Bi alloy solidified under the conditions G = 21.5 K/mm and V = 0.4 μm/s is shown in Figure 6a. The length of α-phase growing (α.f.ℓ), shown in Figure 6b is found to vary with the alloy composition for a constant sample length. The variation of the α-phase fraction versus alloy composition is shown in Figure 7. The calculated values, using the normal freezing equation of solidification, are also plotted in the same figure for comparison. It is seen that the relationship between fs of α-phase vs. composition in the experimental results is analogous to the results of the normal freeze equation.

It is also found that the banded structure can form at growth rates slightly higher than the critical growth rate for a planar α-phase stability. Figure 8 shows the band structures formed at growth rate V = 0.5, 0.55 and 0.6 μm/s at G = 21.5 K/mm conditions for the Pb-30 wt.% Bi alloy. As V = 0.4 μm/s, the α-phase grows as a planar

Figure 5. Band structure morphology at G = 21.5 K/mm and V = 0.4 μm/s for different alloy compositions (in wt.% Bi): a) 24, b) 26, c) 28, d) 30, e) 33, and f) 35

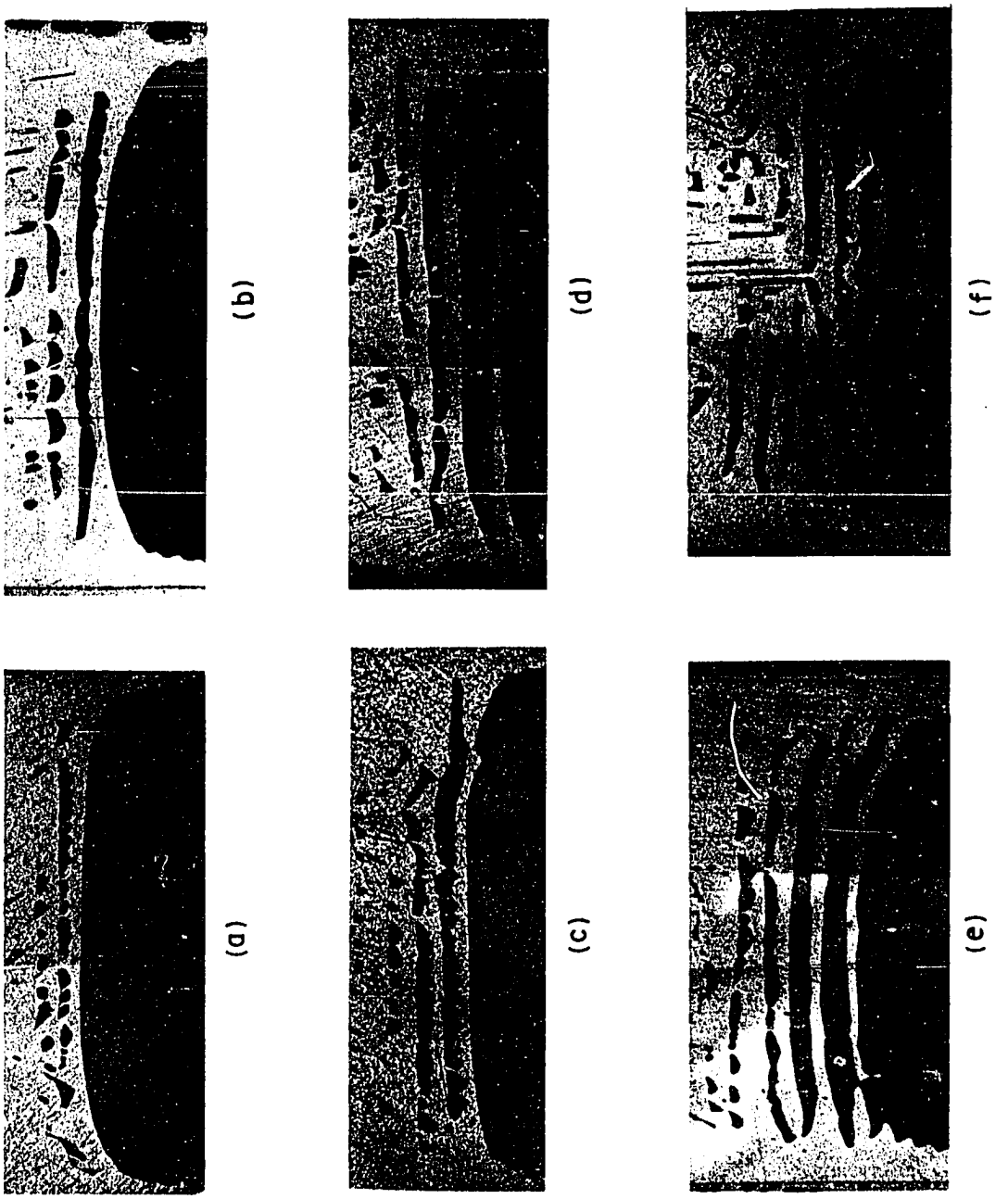
(a)
(b)
(c)
(d)
(e)
(f)

Figure 6. Band formation in the Pb-Bi system.

a) Band structure morphology for Pb-35 wt.% Bi at G = 21.5 K/mm and V = 0.4 μm/s conditions.
b) Schematic band structure for Pb-Bi peritectic alloy under a controlled solidification run

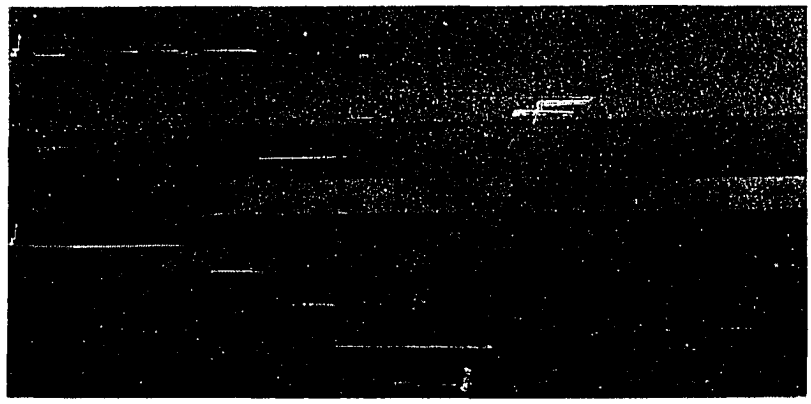

(a)

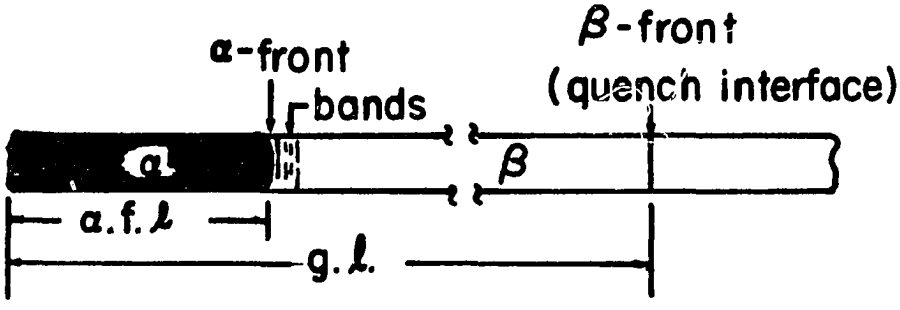

(b)

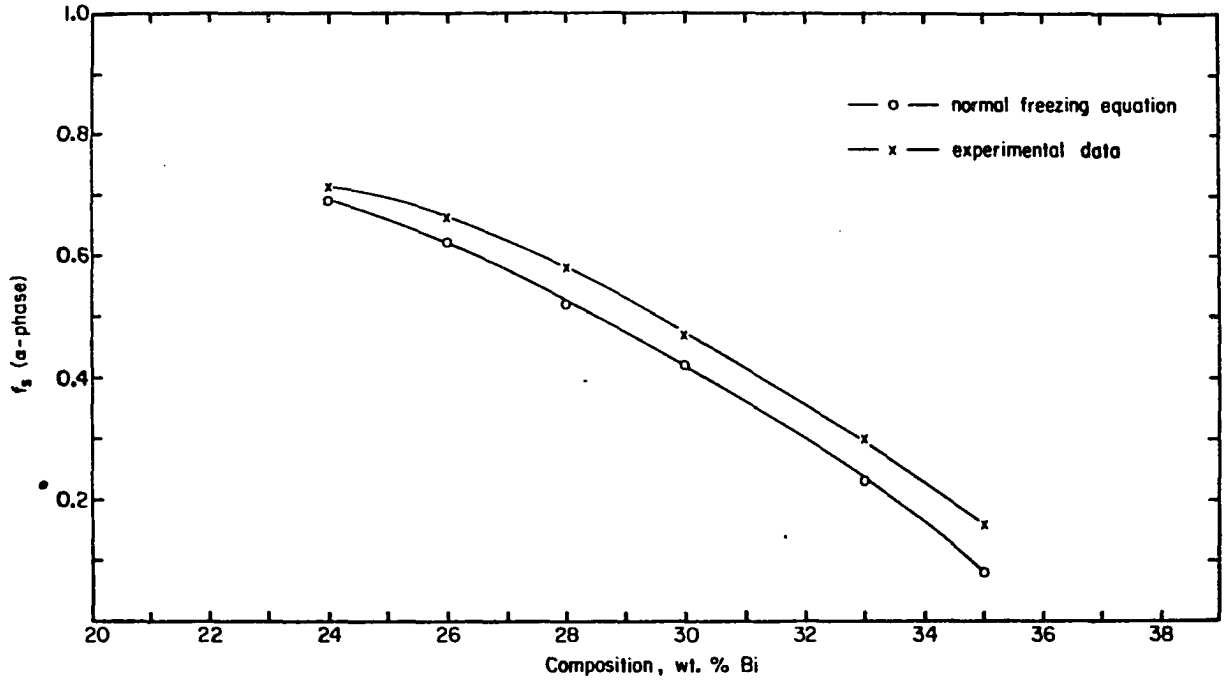

Figure 7. Variation in the fraction α-phase solidified with alloy composition at G = 21.5 K/mm and V = 0.4 μm/s

Figure 8. Band structure obtained at growth rate, V, slightly higher than V_{cr} (= 0.47 μm/s) for Pb-30 wt.% Bi at G = 21.5 K/mm

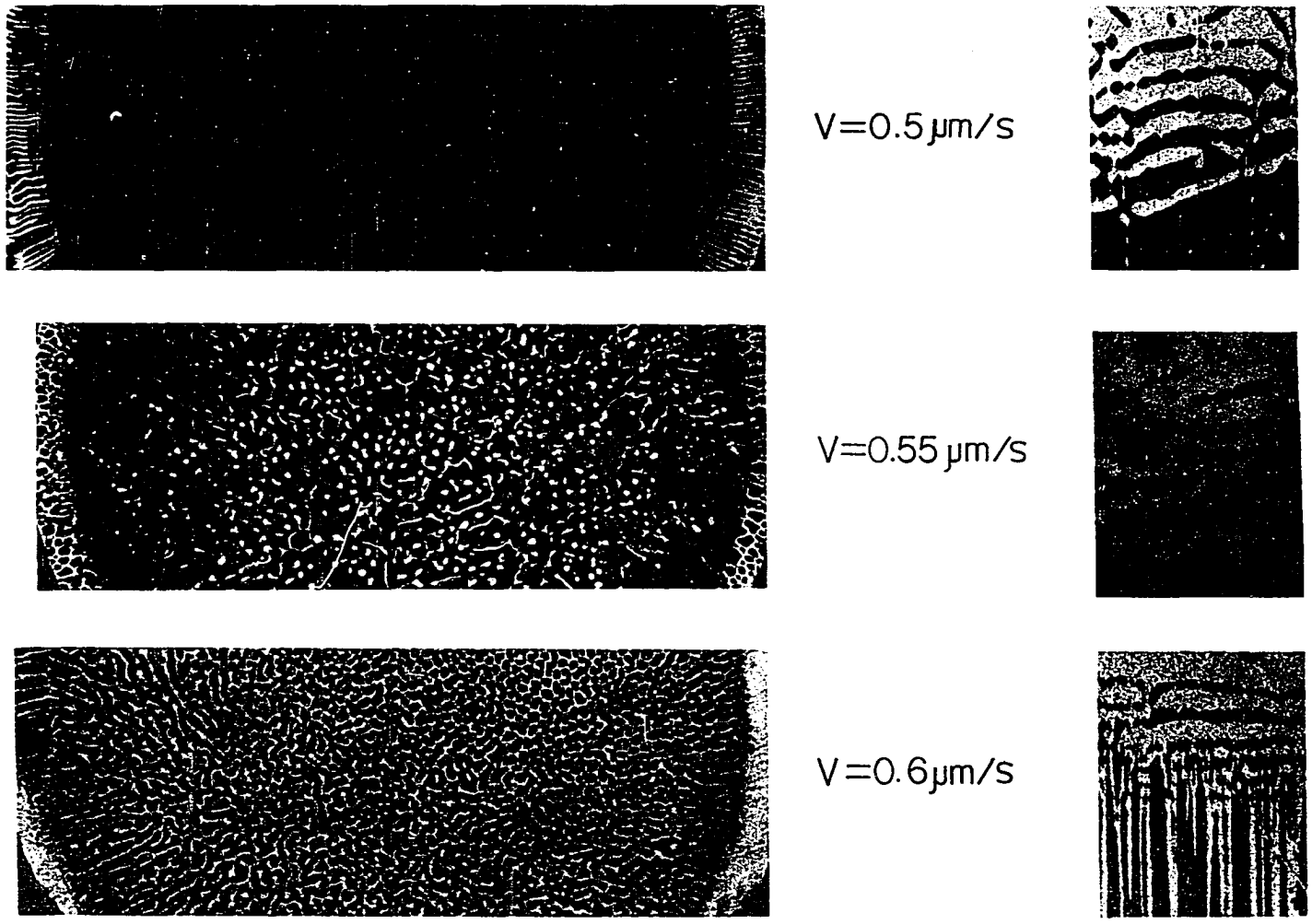
V=0.5 μm/s
V=0.55 μm/s
V=0.6 μm/s
(a)
(b)

interface and it occupied the entire transverse section. When V = 0.5 μm/s, the planar morphology breakup occurs around the outside of the α-phase, as shown in Figures 8 and 9. As V increases again, e.g. V = 0.55 μm/s and 0.6 μm/s, the α-phase breakup is observed over the entire transverse section, and until the α-phase changes to cellular morphology, as shown in Figure 8.

The Pb-28 wt.% Bi alloy, after the controlled solidification run, was chemically analyzed to determine the macrosegregation. The sections location and the results of the analysis are shown in Figure 10. It shows that the concentration along the specimen changes continuously. The macrosegregation occurring along the specimen during solidification process can also be verified by the microstructure morphology changing due to change the growth rate, as shown in Figure 11. The Pb-30 wt.% Bi alloy was grown under G = 21.5 K/mm and V = 0.4 μm/s conditions about 6 cm long, then the growth rate was changed to 25 μm/s and the β-dendrite were observed to form instead of a planar α-phase. It clearly shows that the concentration in melt before the velocity change is higher than the 36 wt.% Bi during the planar α-phase growth. Experimental data obtained in this section are listed in Table 1.

Figure 9. Longitudinal section of Pb-30 wt.% Bi alloy at G = 21.5 K/mm and V (μm/s) of b) 0.4 and c) 0.5; section at A-A in a)

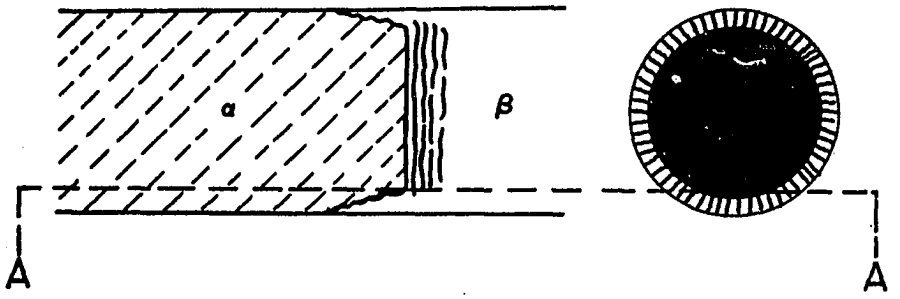

(a)

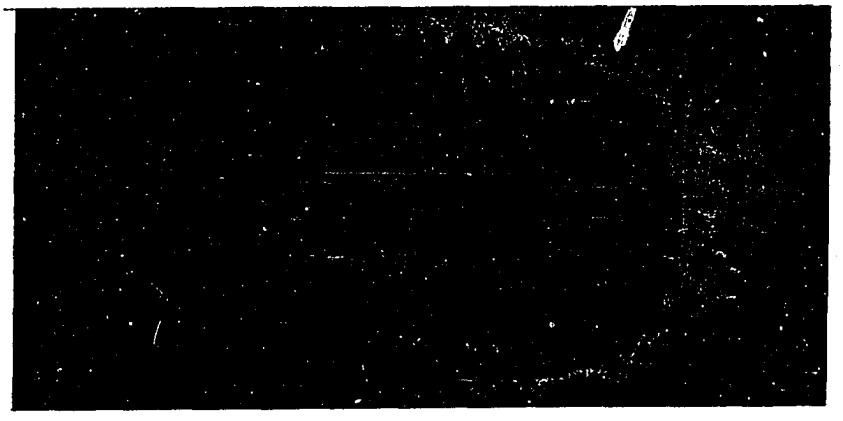

(b)

(c)

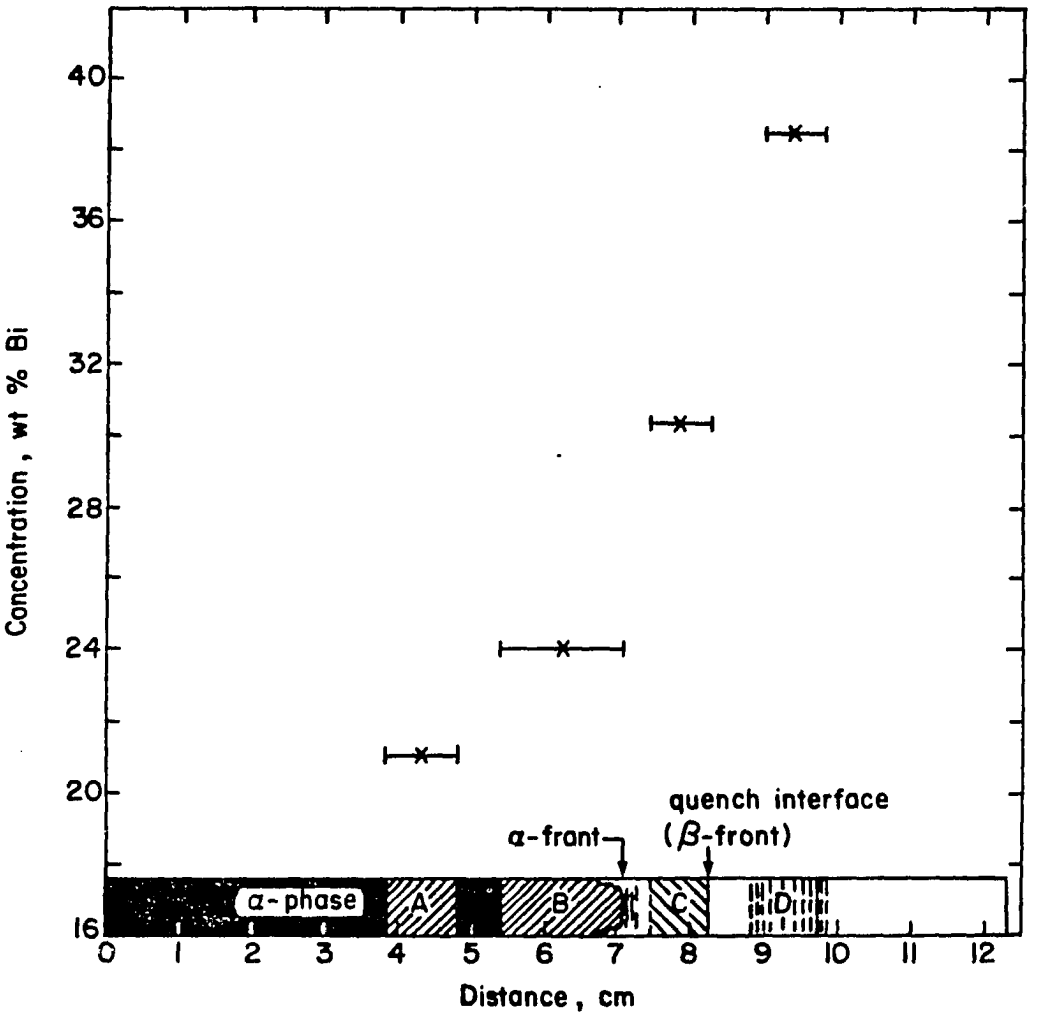

Figure 10. The solute redistribution (macrosegregation) for Pb = 28 wt.% Bi alloy after a controlled solidification (G = 21.0 K/mm, and V = 0.4 μm/s)

Figure 11. The microstructural change from α-planar to β-dendrite by changing the growth rate from 0.4 to 25 μm/s at G = 21.5 K/mm for Pb-30 wt.% Bi alloy. a) Microstructure (M) = 28.54x; b) schematic figure

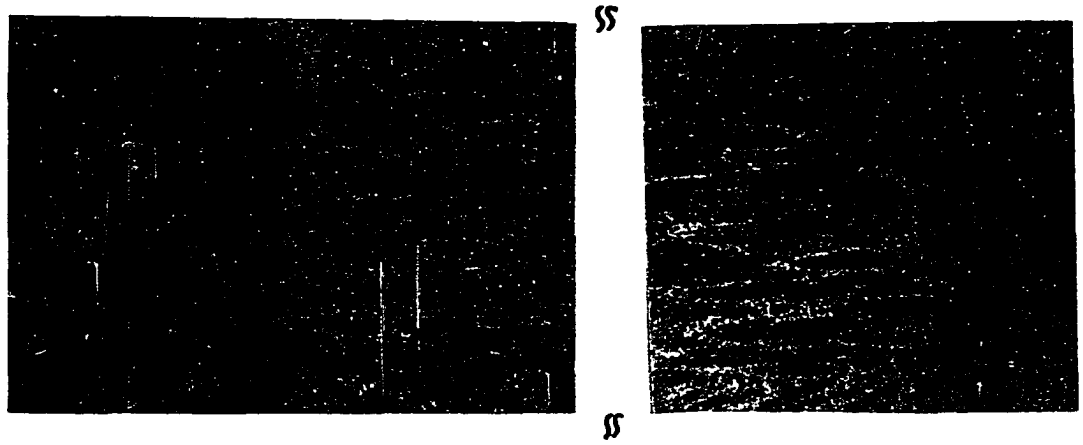

(a)

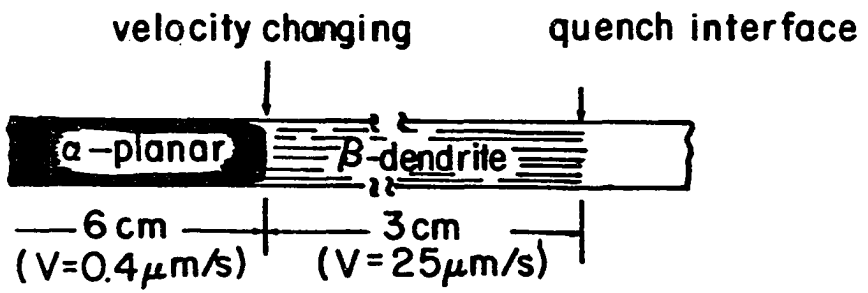
velocity changing
quench interface
α-planar
β-dendrite
6 cm
(V=0.4μm/s)
3cm
(V=25μm/s)

(b)

Table 1. Summary of the band structure experimental data

C (wt.% Bi)	d (g/cm^3)	s.l.[a] (cm)	g.l.[b] (cm)	α.f.l.[c] (cm)	fs (α-phase)
24	10.95	12.27	9.77	8.56	0.71
26	10.91	12.31	8.83	8.12	0.66
28	10.88	12.34	8.25	7.09	0.58
30	10.86	12.39	6.68	5.80	0.47
33	10.81	12.45	6.47	3.75	0.30
35	10.78	12.47	7.71	1.97	0.16

[a] s.l. - specimen length after run.

[b] g.l. - growth length (Figure 6).

[c] α.f.l. - α-phase front length (Figure 6).

[d] Growth conditions: G = 21.5 K/mm; V = 0.4 μm/s.

DISCUSSION

When a Pb-Bi peritectic alloy solidifies with a planar α phase, an alternate band of α and β phases form transverse to the growth direction. There are two phenomena which may contribute to the effect of macrosegregation during growth. One is fluid flow, and the other is thermal transport. Thermal transport should not be significant for growth condition used in this experiment. In the Pb-Bi system, Bi is lighter than lead and so that a density driven convection effect is expected to be present. At a low growth rate, where a planar α phase forms, the rejected solute Bi atoms will be transported in the bulk liquid by diffusion and convection. The bulk liquid concentration will increase along the liquidus of α as well as the composition of the solid α-phase adjacent to the interface will increase along the solidus of α as freezing progresses. Ultimately, the liquid concentration will reach a value equal to, or more probably greater than 36 wt.% Bi, whereupon the peritectic reaction will take place and β phase be nucleated on the α surface. As a consequence, the α surface is covered by β and the subsequent freezing of β from the melt will cause the liquid richer in lead and growth of α can again occur. Such a fluctuant concentration causes the α and β freezing alternately and a band structure formation. Since the interface temperature decreases as the liquid concentration increases, the β phase formation becomes favorable. Finally, only β phase forms as the solidification progresses. The concentration in solid and in liquid will increase continuously as

shown in Figure 10.

Mullins and Sekerka [7] have given a constitutional supercooling criterion equation that if $V_{cr} < GD/\Delta T_o$, a planar interface will be stable with respect to the formation of cells or dendrites. For Pb-30 wt.% Bi alloy, V_{cr} = 0.47 μm/s at G = 21.5 K/mm using D = 1.25 x 10^{-15} cm^2/s. Therefore, as V = 0.50 μm/s, the planar α-phase begins breakup, as shown in Figures 8 and 9.

Boettinger's results, as shown in Figure 1, show the band structures only form in the alloy composition within the hypo-peritectic region (two-phase range) at high G/V values where the planar phase is stable. But in our experiments, the band structure was found to occur over the entire peritectic composition region with the growth rates not only below the V_{cr} value, but also slightly higher than the V_{cr} value, as shown in Figures 6 and 8.

There are two necessary conditions for the normal freeze equation to be valid in solidification process. First, it assumes a complete mixing in the liquid. Second, no diffusion occurs in the solid phase. From Figure 7, it is seen that the results of experiment are similar to the calculated value from the normal freeze equation. This result indicates that strong convection effects are present during the directional solidification studies carried out under low velocity condition.

CONCLUSIONS

1. The band structure is found to occur over the entire peritectic composition region in the Pb-Bi system.

2. The band structure occurs as a transition structure from single α-phase to single β-phase due to the fluctuant concentration in liquid at the solid-liquid interface near the peritectic isotherm.

3. The band structures are observed not only at the velocity below the V_{cr} where the planar α-phase is stable, but also at the velocity slightly higher than V_{cr}, a cellular α-phase forms.

4. Strong convection effects in liquid are found to be present under low velocity conditions where band formation generally occurs.

REFERENCES

1. Boettinger, W. J. Met. Trans. Sept. 1974, 5, 2023.

2. Barker, N. J. W. and Hellawell, A. Met. Sci. 1974, 8, 353.

3. Brody, H. D. and David, S. A. Int. Conf. Solidification and Casting, Sheffield, July 1977, 1, p. 144.

4. Ostrowski, A. and Langer, E. W. Int. Conf. Solidification and Casting, Sheffield, July 1977, p. 139.

5. Titchener, A. P. and Spittle, J. A. Acta Met. April 1975, 23, 497.

6. Hillert, M. Int. Conf. Solidification and Casting, Sheffield, July 1977, 1, p. 81.

7. Mullins, W. W. and Sekerka, R. F. J. Appl. Phys. 1964, 35, 444.

CONCLUSIONS

In Pb-Bi peritectic alloys, the α to β phase transition has been shown to occur at low growth rates, as well as at high growth rates. The length between the α-phase tip and the β-phase tip is studied as a function of temperature gradient, growth rate, alloy composition and the fraction of solid formed. At a fixed solid fraction, it was found that the length decreases with the decrease in the growth rate at constant temperature gradient and composition. There is a linear relationship between them if α phase grew as a dendrite. However, a sharp decrease is observed when α phase formed with a cellular structure. At constant V and G conditions, the length was found to decrease as the composition was increased. In this case, also a linear relationship was shown to exist between ℓ and C when α phase formed a dendritic structure and a sharp decrease was found when α phase formed as a cell. Furthermore, a linear relationship was found between ln ℓ and ln G for a series of constant V if α phase formed as dendritic structure, whereas a sharp decrease in ln ℓ vs. ln G was observed when α phase formated as cellular structure. If the solidified conditions C, V and G are held constant, the length was found to decrease as the solid fraction was increased. Therefore, there is a critical growth velocity which the α phase and β phase will grow at a same growing front, i.e. if the value of ℓ is equal to zero, under certain solidification conditions. This critical growth rate, V_{cr}, could be described by a relationship, $V_{cr} \alpha G^m C^n$, at a fixed solid fraction. The values of m and n were found to be about

1.07 and 6.27 at fs = 0.57, respectively. The experimental results of the relationship between G/V_{cr} vs. C were found to agree with the theoretical model which predicted the planar single β phase stability.

The characteristics of primary spacing for lead-bismuth peritectic alloys are found to be the same as those in eutectic systems. An empirical relationship $\lambda \alpha G^{-a} V^{-b}$ has been found at higher growth velocities to hold true. As V is decreased, the spacing tends to become constant and even to begin decreasing. For constant G and V, the effect of composition on primary spacing in the peritectic region was found to be quite small. The effect of convection was found to affect the primary spacing relationship at low velocities.

In Pb-Bi peritectic alloys, the band structures have been found within the whole peritectic composition regime when the growth conditions were such that the α phase formed as a planar growth front. Band structures were also observed when the conditions were slightly greater than the critical conditions for the planar α phase formation. The band structures were shown to be transition structures when the α phase tends to transform to the β phase at low growth rate conditions. The distance over which the band structures form have been found to decrease as the peritectic alloy composition increased. The composition variation in liquid during the band formation could be described by a normal freeze equation which indicates a strong effect of convection in liquid.

REFERENCES

1. Uhlmann, D. R. and Chadwick, G. A. Acta Met. Sept. 1961, 9, 835.

2. Barker, N. J. W. and Hellawell, A. Met. Sci. 1974, 8, 353-356.

3. Kerr, H. W., Cisse, J. and Bolling, G. F. Acta Met. June 1974, 22, 677-686.

4. Titchener, A. P. and Spittle, J. A. Met. Sci. 1974, 8, 112.

5. Tiwari, S. N., Rao, S. V., Malhotra, S. L. and Misra, S. Scripta Met. 1972, 6, 317.

6. Fredriksson, H. Met. Sci. March 1976, 77.

7. St. John, D. H. and Hogan, L. C. Acta Met. 1977, 25, 77.

8. Boswell, P. G., Chadwick, G. A., Elliott, R. and Sale, F. R. Int. Conf. Solidification and Casting, Sheffield, July 1977, 2, 12 pp.

9. Goddard, D. M. and Childs, W. J. J. of the Less-Common Metals, 1978, 58, 217.

10. Shcherbakov, G. I., David, S. A. and Brody, H. D. Scripta Met. 1974, 8, 1239.

11. Galushko, I. M. Russian J. of Phys. Chem. 1981, 55(2), 184-186.

12. Niwa, K., Shimoji, M. and Mikuni, O. Trans. JIM 1961, 2.

13. St. John, D. H. and Hogan, L. M. J. of Met. Sci. 1982, 17, 2413-18.

14. Galushko, I. M., Taran, Yu N., Klenina, S. Ya and Lisitsa, E. P. Russ. Metall. 1980, 2, 169-173.

15. Chalmers, B. Physical Metallurgy. John Wiley and Sons, Inc., New York, Second printing, 1962, Chapter 6, p. 231.

ACKNOWLEDGMENTS

I would like to express my sincere appreciation and thanks to Dr. R. Trivedi, my major adviser, who gave me an opportunity to pursue this study. Dr. Trivedi has given me valuable advice, prompt assistance, and support which I deeply appreciate.

I would like to thank Dr. J. D. Verhoeven, who gave me many useful suggestions and advice on this dissertation. I would also like to extend my gratitude to Dr. O. N. Carlson, Dr. H. F. Franzen and Dr. T. D. Wheelock who served as my committee members and gave me their support.

I appreciate the assistance that Associate Metallurgist J. Mason gave me in experimental part of this research. I also appreciate all my groupmates for their friendship and the help they provided me in discussing problems.

Sincere thanks go to all my professors who taught me the courses at Iowa State University. Due to their wonderful teaching, I have gotten so much that I did not understand before.

I would like to thank Ms. Barbara Dubberke for her excellent typing and her efforts to meet all the deadlines for this dissertation.

I also would like to express my sincere appreciation to my government, Republic of China in Taiwan, for its support during my studies in America.

Finally, I wish to give a special acknowledgment with deep appreciation to my parents, wife and children, whose love, sacrifices, understanding and encouragement were essential ingredients during my studies in America.